

Dear Paul,

Thanks for doing this review, for your thorough reading of our manuscript and for your positive comments. The points you raised were mindful and certainly helped improving this manuscript. Below, please find your original comments in blue and our responses in black. When referencing page and line numbers, we are always referring to the new versions of manuscript and SI, which are attached at the end. Concerning the literature cited in this answer to your review, we ask you to refer to the attached new version of the manuscript with tracked changes.

General Comments

This is a very well executed, and fairly comprehensive study of ice nucleating particles in the Cape Verde region, especially novel in including measurements in all water and air compartments, and attempting to relate these meaningfully. Overall I had only few comments of significance, and the rest are mostly editorial notes. Specific questions/comments for addressing before publication are listed below.

Specific Comments

1) Abstract, last sentence: I struggled to understand this sentence, although I think it is saying that unless there is an unusual SSA INP emission mechanism in the study area, the INPs cannot be from SSA. But the use of the phrase "unless there would be" seems to beg a question that I thought the papered endeavored to answer. As I read, it seems inconceivable. Or are you referring to situations that you did not measure? I suggest thinking about rewording this sentence.

We changed last sentence in the abstract such that this should be clear now:

“This latter conclusion still holds when accounting for an enrichment of organic carbon in super-micron particles during sea spray generation as reported in literature.”

2) Intro, page 2, line 8: A minor note, since it is not relevant for the main topic of this paper. It is difficult to encapsulate this discussion that seems to be required for every INP paper, but this statement does not reflect any role for INP at temperatures lower than -38 C, which is not the case.

Thanks for your comment. We changed it as:

“Ice crystals in the atmosphere can be formed either via homogeneous nucleation below $-38\text{ }^{\circ}\text{C}$ or via heterogeneous nucleation aided by aerosol particles known as ice nucleating particles (INPs) at any temperature below $0\text{ }^{\circ}\text{C}$.”

3) Intro, page 2, line 28: Higher than ambient INP concentrations at ground level?

Yes, it is. We extended this sentence as:

“Schrod et al. (2017) found that mineral dust or a constituent related to dust was a major contributor to N_{INP} of the aerosol on Cyprus, and N_{INP} in elevated dust plumes was on average a factor of 10 higher than N_{INP} at ground level, where the dust loading is lower.”

4) Intro, page 2, line 29: I do not understand the meaning of, nor see the need for, the ending phrase of this sentence (i.e., : : from the biosphere). It is clear that most INPs come from the biosphere, and the ocean source comes in the form of sea spray aerosol emissions. I favor being explicit.

We deleted this ending phrase “which would...”.

5) Intro, page 2, line 33: Bigg suggested that INPs were contributed to at least some extent from marine emissions, in the data collected in that region at that time. His abstract statement reads that it is not feasible that they are “only of continental origin.”

You are correct in that Bigg (1973) suggested that the INPs are not only of continental origin, but he does not mention marine sources at all. Instead, he argues that there should be a stratospheric source. As the second review suggested, the text in our manuscript was changed to:

“Based on a long-term measurement of INPs in the marine boundary layer in the south of and around Australia, Bigg (1973) suggested that INPs in ambient air were from a distant land source, or from a stratospheric source, and brought to sea level by convective mixing. Schnell and Vali. (1976) suggested a marine source could explain the observations of Bigg (1973).”

6) Intro, page 3, lines 10-11: This is an oft-misinterpreted point. These papers parameterize INPs following this segment of the aerosol population, especially in the free troposphere, but the intention is to reflect INPs at all sizes. It is simply a hook to these concentrations, not intended to represent an actual “fraction” of them.

Thanks for clarifying this. We reworded this sentence.

“Simultaneous measurements of N_{INP} and particle number size distributions were used to develop parameterizations in which N_{INP} depends on a temperature dependent fraction of all particles with sizes above 500 nm (DeMott et al., 2010, 2015).”

7) Intro, page 3, lines 16: Perhaps add qualifier that these observations were in the Arctic “boundary layer”. I bring this up a few times because many things could differ in the free troposphere and at the level of some colder clouds.

It was changed to:

“Creamean et al. (2018) also found that super-micron or coarse mode particles are the most proficient INPs at warmer temperatures in the Arctic boundary layer and they might be biological INPs.”

8) Experiment and Methods, page 4, line 13: The filter sampler was truly sitting at ground level at MV? Or what was the elevation of the sample head? E.g., 1 m above ground?

The filter sampling was done using a Digital filter sampler. The filter head was about 2 m above ground level. As mentioned in the paper, the height of MV is 744 m and the inlet height is 746 m.

We added:

“... on the ground with the inlet 2 m above the bottom, ...”

9) Experiment and Methods, page 5, line 19: Notes on Table S2. The volumes listed do not seem to work out with other information provided, and the header units seem wrong. First, is duration actually in minutes instead of hours? Also, is std volume (must be L, not L-1) for the 2 cm² surface stated as taken? It does not quite make sense, since if this represented 1/100 of the volume flow of

500 lpm, then about 10 times this volume should have been represented. Please fix header units at least. And state in table description if volume is for the "punch" or the total filter. I will revisit this in the next comment.

Thanks a lot for discovering these errors.

The "Duration" should be in minutes. The "Total Volume" should be in std m³ and "Volume Per Well" should be in std L. The volume is always given in standard temperature and pressure (0 °C and 1013.25 hPa).

10) Experiment and Methods, page 6, lines 24-25: So if I have it correct, this amounts to about 0.75 cm² of the filter surface area (96, 1 mm punches). Yet this area is stated as 2 cm² in the previous section. And these new numbers still do not seem to work out to give the sample volumes stated in the tables. I ask these things only if someone wanted to reproduce such work.

For the here presented measurements, only a small piece of 2 cm in diameter was used, from the much larger filter. From this small piece, then pieces with 1 mm in diameter were punched out. The area of these 1 mm needs to set into relation with the size of the overall sampled area. For the filters with diameters of 150 mm, the effective sampling area had a diameter of 140 mm. We made this clearer in the text:

"on 150 mm in diameter quartz fiber filters (Munktell, MK 360) with an effective sampling area of 140 mm in diameter."

"...a circular piece of these filters of 2 cm in diameter was used from which then smaller pieces were punched out for the analysis (see section 2.2)."

11) Experiment and Methods, Section 2.3.2, page 7: Was background testing also done for the other collections, for example by rinsing clean plates use for microlayer sampling and by rinsing the bottles used for seawater collection? Just looking for a few words.

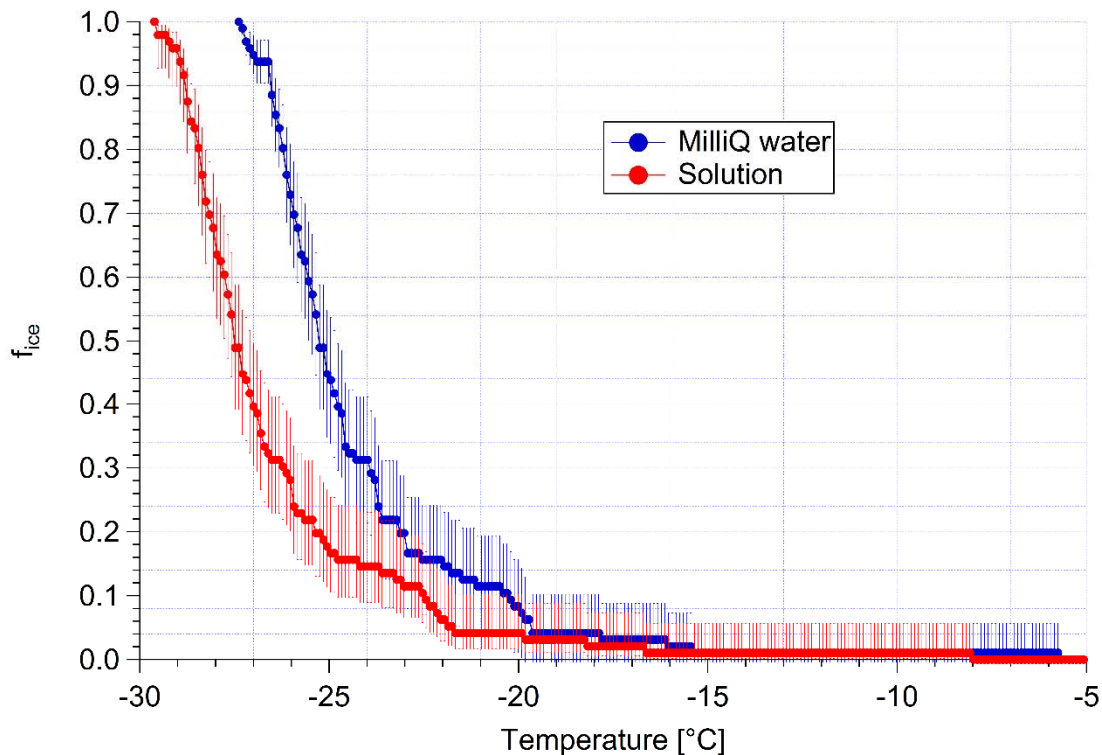
We tested the MilliQ water at Cape Verde and it was as clean as MilliQ water at TROPOS. But we did not test the MilliQ water after washing these glass plates and the containers in which the samples were stored. But we at least explicitly say now, at the end of this section:

“For those samples that were already collected in a liquid state (ULW, SML and cloud water), a background correction was not done.”

12) Experiment and Methods, Section 2.3.3, page 8: I am curious if this calculation of freezing point depression was checked for validation, by for example diluting a seawater sample?

We did not test the freezing point depression previously, but did it now. Since the seawater samples are no longer available, we tested the freezing depression of a pure sodium chloride solution.

We dissolved 0.72 g sodium chloride in 20 mL MilliQ water to get a solution with a salinity similar to that of the SML and ULW samples. The frozen fraction (f_{ice}) of MilliQ water and of this sodium chloride solution are shown in the figure below. The error bars show 95% confidence intervals of f_{ice} . Due to large measurement uncertainties for the first frozen droplets, the freezing point depression should rather be determined from temperatures below approx. $-25\text{ }^{\circ}\text{C}$, where, indeed, a freezing point depression temperature about $\sim 2.2\text{ }^{\circ}\text{C}$ was observed. It is therefore acceptable to use a freezing point depression of $2.2\text{ }^{\circ}\text{C}$ in this study.



13) Experiment and Methods, Section 2.4, page 8: When introducing surface active site density (the terminology I am used to it being referred to as), it could be good to mention already the fact that when applying it to the total aerosol distribution, this artificially assumes that all particles are the same INP type in the contained surface area. This is distinct from a laboratory scenario of generating a specific aerosol, and so will fold in all of the influences present in ambient air.

We followed your suggestion and extended this part as:

“For cases where a single type of aerosol, such as one type of mineral dust, is examined in laboratory studies, A_{total} can be the total particle surface area. However, when field experiments are done, using the total particle surface area of the atmospheric aerosol assumes that all particles contribute to INP and have the same n_s , while the vast majority of these particles will not even be an INP. On the other hand, singling out the contribution of separate INP types in the atmospheric aerosol and relying n_s only to them by using their contribution to the total surface area is at least demanding if not often impossible. This has to be kept in mind when interpreting heterogeneous ice nucleation in terms of n_s ”

14) Results, page 13, lines 5-6: If bio-INPs, the size range is a bit unexpected for marine bacteria, which tend toward micron or less sizes I think. This might support that the bioaerosols are coming from long distance. It also strikes me that a mention for future work might be to include a collection at >2.5 microns, as one wonders about details of the INP size distribution.

We followed your suggestion and added:

“This suggests that these biological INPs might originate from long-range transport, as marine biological INPs were usually reported to be submicron in size (Wilson et al., 2015, Irish et al., 2017). The contribution of SSA to INPs will be discussed further in section 3.4.”

15) Results, page 13, line 12 and Fig. 6: It is not optimal that clouds impacted most of the filters without control, for example by shutting off the pumps, though one understands that clouds are likely pervasive there. This is interpreted as INPs being captured into cloud droplets, and this is supported, but not fully clear. I was struck in Figure 6 by the fact that the CVAO INP

concentrations in 6b all appear higher during cloudy periods in comparison to the couple of periods in Fig. 6a with fewer clouds. Any ideas on why this is so?

There is only a small number of samples. It is seen that during marine events, N_{INP} is lower than during the other times, even up to high ice nucleation temperatures. It is also seen that the cloud free times occurred during the marine times. However, we did not find a good correlation between coarse mode particle number concentration and N_{INP} . These are interesting observations, indeed. But as we only have this very low number of samples collected during the marine period, we not expand on this topic in the text.

The elevation of INP concentrations is over an order of magnitude in a few cases with the largest humps. This is unusual, but also makes me ask if the conclusions about capture of INP into cloud droplets is the full reason for differences below and within cloud. One factor could be drizzle and precipitation. It should be mentioned are solid if clouds were clearly not drizzling, as this could remove or redistribute INPs.

In the companion paper, we characterized the cloud events at MV by comparing the PNSDs at CVAO and MV. The cloud events are pervasive at MV. During the cloud events, most accumulation mode and partly also Aitken mode particles were activated to cloud droplets. We did not have a functioning APS at MV, therefore we cannot compare the coarse mode particles. However, we can assume that most coarse mode particles were activated to cloud droplets because larger particle are easier to activate. INPs are mainly in the super-micron size range, which can explain why most INPs were captured by cloud. There was no precipitation observed at the foothill, which means cloud droplets instead of drizzling were present on the mountaintop.

16) Results, page 14, line 1: Do you discuss cloud diameters in that companion paper? If not, is it consistent with some inference to cloud droplet distributions? This seems to require statement at this point, not later only on page 16.

We did not discuss cloud droplet diameters in the companion paper. But we now added the following in page 15 lines 4-6:

“These observations are consistent with results by Siebert and Shaw (2017) who observed broad cloud droplet size distributions in a size range from ~ 5 to $25 \mu\text{m}$ in shallow cumulus clouds, with the maximum of the distribution still being below $10 \mu\text{m}$.”

17) Results, page 16, lines 21-24: It is not stated explicitly, but it seems clear that for this study, the clouds tended toward relatively high water content for marine Cu, with the lowest values equivalent to the assumptions of Petters and Wright, and the highest values exceeding Rangno and Hobbs. This is just a comment. Drop sizing or LWC measurement would be quite useful in any future studies of this type.

In this study, the LWC was calculated from Equation 6. In this function, we assumed droplet size varies between 7 and 20, with a median value of $15 \mu\text{m}$. Our calculation of the LWC is indeed sensitive to the droplet size. However, with the assumption of a range from 7 to $20 \mu\text{m}$, we can safely assume to cover all possible values of the LWC. As you mentioned, measuring droplet size or LWC would be very helpful in these kinds of study.

18) No reply needed, just to note that the agreement shown in Fig. 8 is striking, even stunning. Also, the discussion at the end of the Results section regarding Fig. 9 is excellent.

Thanks for saying that!

19) Discussion, page 20, lines 1-2: The referenced results for the lack of an influence of SSA on INPs is for a completely different location. I am not sure of the relevance of comparing the two studies other than to note that they concluded the same thing. Are you trying to say the SSA INPs never dominate? I would reject that notion. The only commonality in the two regions is that land sources are present at distances within a day or two trajectory distance. This is not the case everywhere.

The sentence might have been misleading, as it was not meant to say that SSA INPs never dominate. We changed it such that this should be clear now:

“This is in line with results from Si et al. (2018) and Irish et al. (2019a), both done in the Arctic, where it was also concluded that SSA only contributed little to the INP population. The commonality of these two studies from the Arctic and the present study is that land was still close enough so that terrestrial sources can have contributed to the observed INPs.”

20) Discussion, page 20, lines 3-4: How does one know what maximum T desert dust is active? Doesn't this study suggests that -10C is not unreasonable?

You are correct in that there is no maximum T for the activity of desert dust particles. But we also cannot claim the opposite. As the second review suggested, samples CVAO 1596, CVAO 1641 and CVAO 1643 were heated to 95 °C for 1 hour and a large reduction of N_{INP} was observed. Therefore, this paragraph was changed to:

“While the above arguments suggest that INPs in our study were mostly mineral dust particles, there were also some measurements with comparably high INP concentrations at temperatures of -10 °C and above. Although it cannot be ruled out that desert dust particles might be ice active at such high temperatures, by examining the reaction of some highly ice active samples to heating, described in Sec. 3.2.1, we found that the most highly ice active INPs on these samples were biological particles. It is an open question where these biological INPs originated. The times during which these highly ice active INPs were observed were times when air masses came from Southern Europe, travelling along the African coast and meanwhile crossing over the region of the Canary Islands. Therefore, for these specific samples, a contribution of INPs from these land sources might be assumed. ”

21) Discussion, page 21, lines 5-6: Is this too prominent a question? Perhaps, but perhaps not. In regions where marine and dust populations strongly intersect, and both populations contribute to the surface area, it seems that it will ultimately be necessary to parse out the contributions. This was not done in DeMott et al. (2016), and that probably makes inclusion of those data as purely SSA somewhat suspect for the data collected in the Caribbean, especially. It makes it difficult to discern anywhere, if a few percent of dust by number is sometimes present (a few papers on this are in press). Do you have any compositional inferences to use here? Consider figures 4 and 5 for

of Gong et al. (2019a) for varied compositions during different times. Do the numbers roughly work out if you assume something to use as pure dust? You do not really dig into this at all. It may be a major question, but you appear to have some additional information that would allow you to state if your data are consistent with the proportions of mineral and marine particles.

Thanks for your comment. It is really interesting for the future work to parse out the SSA and dust contribution to INPs at Cape Verde. Since we have classified the particle types in the companion paper, we can compare the n_s during marine and dust periods. We added the following in page 22, line 3:

“CVAO is a place where marine and dust particles strongly intersect, and both particle types contribute to the surface area. In the companion paper, we have classified the aerosol at CVAO into four different types. Here, in addition to looking at average values as presented above, we selected the most clean marine (CVAO 1585) and most dusty (CVAO 1591) samples for a separate calculation of n_s and added the results to Fig. 9. The n_s is clearly higher for the sample collected during the dusty period than during the marine period at higher temperatures (roughly >-16 °C). However, at temperatures below -18 °C it is the other way around. In general, results for these vastly different cases are both still close to the upper limit of the parameterizations reported for SSA.

These comparisons to literature raise the question if and how n_s should be used to parameterize atmospheric INP measurements, which, however, is a question far too prominent to be answered in this study. In general, it is still an open issue to which extent N_{INP} can be parameterized, based on one or a few parameters, to reliably describe N_{INP} for different locations around the globe. It might prove necessary to develop separate parameterizations for different locations or air masses, as it was already started for parameterizations based on particle number concentrations (see e.g., DeMott et al. (2010); Tobo et al. (2013); DeMott et al. (2015)).”

22) Summary and Conclusions, page 21, lines 19-20: The sentence is not complete, and it is unclear if it is referring to other studies or this one. If referring to this study, I suggest to say that “biological particles appeared to contribute: :” I note though that no confirmatory tests were performed to ascertain biological INP influence.

You were right about the confirmatory tests, which now were added, as said before: Samples CVAO 1596, CVAO 1641 and CVAO 1643 were heated to 95 °C for 1 hour and a great reduction of N_{INP} was observed. This sentence was changed to:

“These elevated values disappeared after heating the samples at 95 °C for 1 hour. Therefore, biological particles appear to contribute to INPs at these moderate supercooling temperatures.”

Reference:

Bigg, E. K.: Ice Nucleus Concentrations in Remote Areas, *Journal of the Atmospheric Sciences*, 30, 1153-1157, doi:10.1175/1520-0469(1973)030<1153:INCIRA>2.0.CO;2, 1973.

Siebert, H., and Shaw, R. A.: Supersaturation Fluctuations during the Early Stage of Cumulus Formation, *Journal of the Atmospheric Sciences*, 74, 975-988, 10.1175/jas-d-16-0115.1, 2017.

Characterization of aerosol particles at Cape Verde close to sea and cloud level heights - Part 2: ice nucleating particles in air, cloud and seawater

Xianda Gong¹, Heike Wex¹, Manuela van Pinxteren¹, Nadja Triesch¹, Khanneh Wadinga Fomba¹, Jasmin Lubitz¹, Christian Stolle^{2,3}, Tiera-Brandy Robinson³, Thomas Müller¹, Hartmut Herrmann¹, and Frank Stratmann¹

¹Leibniz Institute for Tropospheric Research, Leipzig, Germany

²Leibniz-Institute for Baltic Sea Research Warnemünde (IOW), Rostock, Germany

³Institute for Chemistry and Biology of the Marine Environment, University of Oldenburg, Wilhelmshaven, Germany

Correspondence: Xianda Gong (gong@tropos.de)

Abstract. Ice nucleating particles (INPs) in the troposphere can form ice in clouds via heterogeneous ice nucleation. Yet, atmospheric number concentrations of INPs (N_{INP}) are not well characterized and although there is some understanding of their sources, it is still unclear to what extent different sources contribute, nor if all sources are known. In this work, we examined properties of INPs at Cape Verde from different [sources/compartments](#), the oceanic sea surface microlayer (SML) and underlying water (ULW), the atmosphere close to both sea and cloud level as well as cloud water.

Both enrichment and depletion of N_{INP} in SML compared to ULW were observed. The enrichment factor (EF) varied from roughly 0.4 to 11, and there was no clear trend in EF with [ice nucleation](#) temperature.

N_{INP} in PM_{10} sampled at Cape Verde Atmospheric Observatory (CVAO) at any particular [ice nucleation](#) temperature spanned around 1 order of magnitude below $-15\text{ }^{\circ}\text{C}$, and about 2 orders of magnitude at warmer temperatures ($>-12\text{ }^{\circ}\text{C}$). N_{INP} in PM_1 were generally lower than those in PM_{10} at CVAO. About $83\pm 22\%$, $67\pm 18\%$ and $77\pm 14\%$ (median \pm standard deviation) of INPs had a diameter $>1\text{ }\mu\text{m}$ at ice [activation/nucleation](#) temperatures of -12 , -15 , and $-18\text{ }^{\circ}\text{C}$, respectively. Among the 17 PM_{10} samples at CVAO, three PM_{10} filters showed elevated N_{INP} at warm temperatures, e.g., above 0.01 std L^{-1} at $-10\text{ }^{\circ}\text{C}$. [After heating samples at \$95\text{ }^{\circ}\text{C}\$ for 1 hour, the elevated \$N_{\text{INP}}\$ at the warm temperatures disappeared, indicating that these highly ice active INPs were most likely biological particles.](#) However, ~~for N_{INP} in PM_1 at CVAO, this is not the case.~~ PM_1 at CVAO ~~did not show such elevated N_{INP} at warm temperatures.~~ ~~At these higher temperatures, often biological particles have been found to be ice active.~~ Consequently, the difference in N_{INP} between PM_1 and PM_{10} at CVAO suggests that biological ice active particles were present in the super-micron size range.

N_{INP} in PM_{10} at CVAO was found to be similar to that on Monte Verde (MV, at 744 m a.s.l) during non-cloud events. During cloud events, most INPs on MV were activated to cloud droplets. When highly ice active particles were present in PM_{10} filters at CVAO, they were not observed in PM_{10} filters on MV, but in cloud water samples, instead. This is direct evidence that these INPs which are likely biological are activated to cloud droplets during cloud events.

In general, Cape Verde was often affected by dust from the Saharan desert during our measurement. For the observed air masses, atmospheric N_{INP} in air fit well to the concentrations observed in cloud water. When comparing concentrations of both sea salt and INPs in both seawater and PM₁₀ filters, it can be concluded that sea spray aerosol (SSA) only contributed a minor fraction to the atmospheric N_{INP} . ~~Therefore it can be said that, unless there would be a significant enrichment of N_{INP} during the formation of SSA particles, N_{INP} was mainly dominated by mineral dust at cold temperatures with few contributions from possible biological particles at warmer temperatures.~~ This latter conclusion still holds when accounting for an enrichment of organic carbon in super-micron particles during sea spray generation as reported in literature.

1 Introduction

Ice particle formation in tropospheric clouds can affect cloud properties such as cloud lifetime, their radiative effects on the atmosphere, and the formation of precipitation (Hoose and Möhler, 2012; Murray et al., 2012). Ice crystals in the atmosphere can be formed either via homogeneous nucleation below $-38\text{ }^{\circ}\text{C}$ or ~~heterogeneous nucleation aided by aerosol particles known as ice nucleating particles (INPs) at warmer temperatures ($> -38\text{ }^{\circ}\text{C}$)~~ via heterogeneous nucleation aided by aerosol particles known as ice nucleating particles (INPs) at any temperature below $0\text{ }^{\circ}\text{C}$. Immersion freezing refers to the process when an INP becomes immersed in an aqueous solution e.g., through the process of cloud droplet activation (Vali et al., 2015). Immersion freezing is suggested to be the most important freezing process for mixed phase clouds (Ansmann et al., 2008; Westbrook and Illingworth, 2013), and is the process we will focus on in this study.

~~Dust particles are recognized as effective INPs below $-20\text{ }^{\circ}\text{C}$ (Augustin-Bauditz et al., 2014) or even below $-15\text{ }^{\circ}\text{C}$ (Hoose and Möhler, 2012; Murray et al., 2012).~~ Submicron dust particles are recognized as effective INPs below $-20\text{ }^{\circ}\text{C}$ (Augustin-Bauditz et al., 2014) and super-micron dust particles were reported to be ice active even up to $-10\text{ }^{\circ}\text{C}$ (Hoose and Möhler, 2012; Murray et al., 2012). Laboratory studies on natural mineral dusts from different regions have been conducted to quantify the particle's ability to nucleate ice (Niemand et al., 2012; DeMott et al., 2015). Mineral dust particles from deserts are composed of a variety of minerals, and K-feldspar is supposed to be more ~~effective~~ active for ice nucleation than other minerals in the mixed-phase cloud temperature regime (Atkinson et al., 2013; Augustin-Bauditz et al., 2014; Niedermeier et al., 2015). ~~However, overall, desert dust particles from diverse sources show comparable ice nucleating efficiency (Boose et al., 2016).~~ Boose et al. (2016) found that ice activity of desert dust particles at temperatures between -35 and $-28\text{ }^{\circ}\text{C}$ can be attributed to the sum of the feldspar and quartz content. A high clay content, in contrast, was associated with lower ice nucleation activity. In contrast to field measurements, in laboratory studies often separate types of mineral dusts are examined. Different parameterizations have been employed to summarize the mineral dust particle's ice nucleating ability (Niemand et al., 2012; Ullrich et al., 2017).

A few field measurements have been carried out to quantify the ice nucleation properties of desert dust. Based on airborne measurements, DeMott et al. (2003) found that ice nucleating aerosol particles in air masses over Florida had sources from the North African ~~dust~~ desert. Chou et al. (2011) observed a good correlation between the number concentration of larger particles and INP number concentration (N_{INP}) during a Saharan dust event at the Jungfraujoch in the Swiss Alps. Collecting airborne dust over the Saharan desert, Price et al. (2018) observed two orders of magnitude variability in N_{INP} at any particular

temperature from ~ -13 to ~ -25 °C, which was related to the variability in atmospheric dust loading, ~~while desert dust's ice-nucleating activity was only weakly dependent on the differences in desert sources.~~ This desert dust's ice nucleating activity was only weakly dependent on differences in desert sources, i.e., on the differences in mineral composition that particles emitted from different locations in the desert may have. Schrod et al. (2017) found that mineral dust or a constituent related to dust was a major contributor to ~~the ice nucleating properties~~ N_{INP} of the aerosol on Cyprus, and N_{INP} in elevated dust plumes was on average a factor of 10 higher than N_{INP} at ground level, where the dust loading was lower.

Ocean water can be a potential source of INPs (Brier and Kline, 1959) ~~which would originate from the biosphere.~~ The source of INPs in ocean water might be associated with phytoplankton blooms (Schnell and Vali, 1976). Recently, Wilson et al. (2015) and Irish et al. (2017) found that organic material, with a diameter $<0.2 \mu\text{m}$, is the major ice nucleator in the sea surface microlayer (SML). Based on a long-term measurement of INPs in the marine boundary layer in the south of and around Australia, Bigg (1973) suggested that INPs in ambient air ~~were contributed by marine aerosol particles~~ were from a distant land source, or from a stratospheric source, and brought to sea level by convective mixing. Schnell and Vali (1976) suggested a marine source could explain the observations of Bigg (1973). DeMott et al. (2016) found that ~~INPs~~ the ice nucleation activity from laboratory generated sea spray aerosol (SSA) aligned well with measurements from diverse regions over the oceans. ~~Further evidence of~~ Furthermore, a connection between marine biological activity and N_{INP} was uncovered in their laboratory study (DeMott et al., 2016). In pristine marine conditions, such as the Southern Ocean, SSA was the main source of the INP population, but N_{INP} was relatively low in the Southern Ocean as well as in the clean marine Northeast Atlantic (McCluskey et al., 2018a, b). These field measurements are consistent with the model work by Burrows et al. (2013), which emphasizes the importance of SSA contribution to INPs in remote marine regions.

It is currently still uncertain whether the coarse mode particles or smaller particles are the major source of atmospheric INPs. Vali (1966) found that the diameters of INPs were mostly between 0.1 and $1 \mu\text{m}$. On the high alpine research station Jungfraujoch, Mertes et al. (2007) found that ice residuals were as small as 300 nm and they were mostly present in the submicron particle size range. ~~Modeling studies also suggest that INP are a temperature dependent fraction of all particles with sizes above 500 nm.~~ Simultaneous measurements of N_{INP} and particle number size distributions were used to develop parameterizations in which N_{INP} depends on a temperature dependent fraction of all particles with sizes above 500 nm (DeMott et al., 2010, 2015). Conen et al. (2017) found INPs at -8 °C were equally distributed amongst the particles with sizes up to $2.5 \mu\text{m}$ and with sizes between 2.5 and $10 \mu\text{m}$. Other field measurements reported that coarse mode particles were more efficient INP, e.g., INPs (mainly bacterial aggregates and fungal spores) occurred in the size range of 2 - $6 \mu\text{m}$ (Huffman et al., 2013). Mason et al. (2016) found for Arctic aerosol that $91 \pm 9\%$, $79 \pm 17\%$, and $63 \pm 21\%$ of INPs had an aerodynamic diameter of $>1 \mu\text{m}$ at ice activation temperatures of -15 , -20 , and -25 °C, respectively. Creamean et al. (2018) also found that super-micron or coarse mode particles are the most proficient INPs at warmer temperatures in the Arctic boundary layer and they might be biological INPs. Concerning biological INP, it should be mentioned that it is well understood by now that these feature macromolecules of only some ten nanometers in size at the most (Pummer et al., 2015). Some of them are easily separated from their carrier (e.g., from pollen and fungal spores), while others are embedded in the cell membrane (e.g., for bacteria), ~~but based on these above cited literature results, it seems that most of the biological INPs still occur together with their original carrier in the atmosphere~~ but based on the fact

that most atmospheric INPs seem to be super-micron in size, as observed in the above cited literature, it seems that most of the biological ice active macromolecules still occur together with their original carrier in the atmosphere.

Direct measurement of N_{INP} in the cloud water can be used to estimate concentrations of INPs in the air assuming that most INPs activate as CCN. Joly et al. (2014) measured total and biological (i.e., heat-sensitive) INPs between -5 to -14 °C in cloud samples from the summit of Puy de Dôme (1465 m a.s.l., France). Petters and Wright (2015) summarized many INP spectra obtained from rain water, melted sleet, snow and hail samples at different sampling locations and reported a range of N_{INP} for these precipitation samples. Based on a shipborne measurement of the east coast of Nova Scotia, Canada, Schnell (1977) directly compared N_{INP} in the seawater to that in the fog water and found that N_{INP} in fog water and seawater appeared to vary quite independently of each other. As one part of the here presented study, these field measurement values will be compared with values obtained from our measurement campaign in the framework of the MarParCloud (Marine biological production, organic aerosol particles and marine clouds: a Process Chain) project.

During the MarParCloud project, samples collected for INPs analysis include: SML and underlying water (ULW) from the ocean upwind of the island; quartz fiber filter samples of atmospheric aerosol, collected on a tower installed at the island shore (inlet height: 42 m a.s.l) and on a mountaintop (inlet height: 746 m a.s.l); and cloud water collected during cloud events on the mountaintop. In this study, we will first discuss N_{INP} in the SML and ULW. We will then discuss N_{INP} in the air, including a comparison of N_{INP} in PM_{10} and PM_1 and a comparison of N_{INP} close to both sea and cloud level. Lastly, N_{INP} in the cloud water will be discussed. In addition, we will provide a feasible way to link N_{INP} in ambient air, ocean water and cloud water. This connection can be drawn only during times when there were cloud events on the mountaintop, together with data on number concentrations on cloud condensation nuclei (N_{CCN}). Respective information was derived and discussed in an accompanying paper (Gong et al., 2019b). For more information about the campaign itself, we refer to an upcoming overview paper by van Pinxteren et al.

2 Experiment and methods

2.1 Sampling sites and sample types

2.1.1 Sampling site

~~The measurements were carried out~~The measurement campaign was carried out on São Vicente island at Cape Verde from 13 September to 13 October, 2017. We set up three measurement stations at Cape Verde, at the Cape Verde Atmospheric Observatory (CVAO), on Monte Verde (MV) and an Ocean Station (OS). CVAO ($16^{\circ}51'49$ N, $24^{\circ}52'02$ W) is located in the ~~northwest-~~northeastern shore of the island of São Vicente, 70 m from the coastline about 10 m a.s.l. Filter samplers were installed on top of a 32 m tower. MV ($16^{\circ}52'11$ N, $24^{\circ}56'02$ W) is located on a mountaintop (744 m a.s.l), ~ 7 km away to the west of CVAO. Filter samplers were situated on the ground with the inlet 2 m above the bottom, upwind of any installations on the mountaintop. The OS covered an area at $\sim 16^{\circ}53'30$ N, $\sim 24^{\circ}54'00$ W, with a distance of at least 5 km from the island. Details on the measurement site and the meteorological conditions can be found in the accompanying paper (Gong et al., 2019b). In

short, the conditions at Cape Verde were quite stable, with temperature of on average 26.6 °C at CVAO and 21.2 °C at MV and wind speeds between 0.6 and 9.7 m s⁻¹ with directions from the northeast.

In the following, the different samples collected during the campaign are described in detail. All of these samples were stored at -20 °C right after sampling. After the campaign the long-term storage and transport of the collected samples from Cape Verde to the Leibniz Institute for Tropospheric Research (TROPOS), Germany was carried out in a cooled container at -20 °C. At TROPOS, all samples were again stored frozen at -20 °C until analysis was done. Measurement sites, locations, sample types and additional information are summarized in Tab. 1.

Table 1. Measurement sites, locations, sample types and measurement instruments.

Measurement site	Location	Sample type	Instrument
CVAO	16°51'49 N, 24°52'02 W inlet height: 42 m a.s.l	PM ₁ quartz fiber filter	INDA
		PM ₁₀ quartz fiber filter	INDA
MV	16°52'11 N, 24°56'02 W inlet height: 746 m a.s.l	PM ₁₀ quartz fiber filter	INDA
		Cloud water	LINA, INDA
OS	~16°53'30 N, ~24°54'00 W	SML	LINA, INDA
		ULW	LINA, INDA

Following the description of the sampling, we will briefly introduce the measurement methods related to INPs, including freezing devices, N_{INP} calculation and measurement uncertainties. Note that all the times presented here are in UTC (corresponding to local time +1). For better comparison, all ambient particle number concentrations in this study are given for standard temperature and pressure (STP, 0 °C and 1013.25 hPa).

2.1.2 Seawater sampling

Seawater samples were taken at the OS by using a fishing boat at a distance of at least 5 km from the coast (off-shore samples). The SML samples were collected using a glass plate sampler (Harvey and Burzell, 1972; Irish et al., 2017; van Pinxteren et al., 2017). The glass plate had a surface area of 2000 cm⁻² and was immersed vertically into the ocean and then withdrawn at a slow rate (between 5 to 10 cm s⁻¹) and allowed to drain for less than 5 s. The surface film adhering to the surface of the glass was scraped off from both sides of the glass plate with a framed Teflon wiper into a 1 liter glass bottle. For each SML sample, several liters were collected and 1 liter was required ~55 dips. Based on the amount of material collected, the number of dips and the area of the plate, the averaged thickness of the layer collected was calculated as ~91.0 μm. ULW samples were collected at the same time and location as the SML samples. ULW was collected from a depth of 1 m by a specially designed device, which consists of a glass bottle mounted on a telescopic rod in order to monitor sampling depth. The bottle was opened underwater at the intended sampling depth with a specifically designed seal-opener. After collection, the glass bottles

containing both the SML and ULW samples were kept in a freezer at -20°C up to the analysis. During the campaign, 9 SML and 9 ULW samples were collected for INP analysis. Details of SML and ULW samples, including the sampling time, location, salinity and additional information are provided in the supplement, Tab. S1.

2.1.3 Aerosol particle sampling

5 Particle sampling was done using high-volume samplers with either a PM_{10} -inlet and or a PM_1 -inlet (Digital filter sampler DHA-80, Walter Riemer Messtechnik, Germany) operating with an average flow rate of $\sim 500\text{ L min}^{-1}$ for 24 hours sampling periods. The high-volume samples were collected on 150 mm in diameter quartz fiber filters (Munktell, MK 360) filters with
10 an effective sampling area of 140 mm in diameter. The filters were preheated in our laboratory at 110°C for 24 hours to remove the organic carbon background. After sampling, the filters were transported to a freezer where they were kept at -20
15 $^{\circ}\text{C}$. For INP analysis, a fraction circular piece of these filters of 2 cm² cm in diameter was used from which then smaller pieces
were punched out for the analysis (see section 2.2). From CVAO, there were 17 and 19 filters from PM_{10} and PM_1 collection (CVAO PM_{10} and CVAO PM_1), respectively, and at MV, 17 filters were collected for PM_{10} (MV PM_{10}). Field blind filters were obtained by inserting clean filters into the Digital sampler for a period of 24 hours without loading them. Three blind filters were collected during this campaign. Details of filter samples, including sampling time, duration, total volume and additional
information can be found in the supplement, Tab. S2 (CVAO PM_{10}), Tab. S3 (CVAO PM_1) and Tab. S4 (MV PM_{10}).

2.1.4 Cloud water sampling

During the campaign, MV was in clouds roughly 58% of the time (a detailed analysis on this can be found in Gong et al. (2019b)). Cloud water was collected with CASCC2 (Caltech Active Strand Cloud Collector Version 2) at MV. All cloud drop sizes were collected in one bulk sample. Drops were collected by inertial impaction on Teflon strands with a diameter of 508
20 μm . The 50% lower size cut for the CASCC2 was approximately 3.5 μm diameter. The flow rate through the CASCC2 was approximately $5.8\text{ m}^3\text{ min}^{-1}$. The CASCC2 is described in more details in Demoz et al. (1996). Between cloud events, the cloud water sampler was cleaned with a large amount ($\sim 5\text{ L}$) of ultrapure water. Once the collector was cleaned, a blank was taken by spraying about 200 mL of ultrapure water into the collection strands in the collector and subsequent sampling of this
25 water. After collection, the cloud water samples were kept in a freezer at -20°C . During the campaign, 13 cloud samples were collected for INP analysis. The details of cloud samples, including sampling time, duration, volume and additional information are provided in the supplement, Tab. S5.

2.2 Freezing devices

Two droplet freezing devices called LINA (Leipzig Ice Nucleation Array) and INDA (Ice Nucleation Droplet Array) have been set up at TROPOS in Germany. The design of LINA was inspired by Budke and Koop (2015). Briefly, 90 droplets with the
30 volume of 1 μL were pipetted from the samples onto a thin hydrophobic glass slide, with each droplet being placed separately into its own compartment. After pipetting, the compartments were sealed at the top with another glass slide, to prevent the

droplets from evaporation and to prevent ice seeding from neighboring droplets. The droplets were cooled on a Peltier element with a cooling rate of 1 K min^{-1} down to $-35 \text{ }^\circ\text{C}$, while the setup was illuminated by a circular light source from above. Once the cooling started, pictures were taken every 6 s by a camera. The number of frozen versus unfrozen droplets was derived automatically by an image identification program in Python. LINA was employed to measure SML, ULW and cloud water samples in this study. More detailed parameters and the temperature calibration of LINA and its application can be found in previous studies (Chen et al., 2018; Gong et al., 2019a).

The design of INDA was inspired by Conen et al. (2012), but deploying PCR-trays instead of separate tubes. For quartz fiber filters, circular pieces with a diameter of 1 mm were punched out. Each of the 96 wells of a PCR-tray were filled with the filter piece together with $50 \text{ } \mu\text{L}$ of ultrapure water. For SML, ULW and cloud water samples, $50 \text{ } \mu\text{L}$ of the water samples was filled into each PCR-tray. After sealing by a transparent foil, the PCR-tray was placed on a sample holder and immersed into a bath thermostat, where it was illuminated from below with a LED light source. The bath thermostat then decreased the temperature with a cooling rate of approximately 1 K min^{-1} . Real-time images of the PCR-tray were recorded every 6 s by a CCD (charge-coupled device) camera. Frozen droplets can be identified based on the brightness change during the freezing process. A program recorded the actual temperature of the cooling bath and related it to the real-time images from the CCD camera. The temperature in the PCR-trays had been calibrated. More detailed parameters and temperature calibration of INDA and its application can be found in previous studies (Chen et al., 2018; Hartmann et al., 2019).

2.3 Deriving N_{INP}

2.3.1 Basic calculation

Based on Vali (1971), the cumulative concentration of INP (N_{INP}) as a function of temperature per air or water volume can be calculated by:

$$N_{\text{INP}}(\theta) = \frac{-\ln(1 - f_{\text{ice}}(\theta))}{V} \quad (1)$$

with

$$f_{\text{ice}}(\theta) = \frac{N(\theta)}{N_{\text{total}}} \quad (2)$$

where N_{total} is the number of droplets and $N(\theta)$ is the number of frozen droplets at temperature θ . Eq. 1 accounts for the possibility of the presence of multiple INPs in one vial by assuming that INPs are Poisson distributed. [This way, the cumulative number of INP active at any temperature will be obtained although only the most ice active INP \(nucleating ice at the highest temperature\) present in each droplet/well will be observed.](#) As for the quartz fiber filters, V is the volume of air collected onto one circular 1 mm filter piece placed in each well, resulting in airborne N_{INP} . The information of the air volume can be found in the supplement, Tab. S2, Tab. S3 and Tab. S4. As for the SML, ULW and cloud water, V is the volume of droplet/well ($V_{\text{LINA}}=1 \text{ } \mu\text{L}$, $V_{\text{INDA}}=50 \text{ } \mu\text{L}$), resulting in N_{INP} per volume of water. Compared to the droplets examined in a LINA measurement, INDA measurements have a larger volume of water in each well. The larger volume of water corresponds to a higher probability of

the presence of INPs in each well, therefore INDA can detect INPs at warmer temperatures, where INP are more scarce. In this study, the derived N_{INP} from LINA and INDA measurements were combined when both instruments were deployed.

2.3.2 Uncertainty and background

Because the number of INPs present in the [washing](#) water is usually small (some single up to a few tens of INPs per examined droplet/well), and the number of droplets/wells considered in our measurements is limited, statistical errors need to be considered in the data evaluation. Therefore, confidence intervals for f_{ice} were determined using the method suggested by Agresti and Coull (1998). [These confidence intervals were estimated according to the improved Wald interval which implicitly assumes a normal approximation for binomially distributed measurement errors.](#) Previous studies (McCluskey et al., 2018a; Suski et al., 2018; Gong et al., 2019a) used the same method to calculate the freezing devices' measurement uncertainties.

For the quartz fiber filters, a background freezing signal resulting from the field blind filters was determined by doing a regular INDA measurement with these filters. Measured N_{INP} from the sampled filters was corrected by subtracting the averaged background concentrations determined for the blind filters. ~~A detailed explanation of background subtraction can be found in the supplement of, as explained in~~ Wex et al. (2019). All values for airborne N_{INP} presented in the following are background-corrected. [A detailed description of the background subtraction method and background values are provided in the supplement. For those samples that were already collected in a liquid state \(ULW, SML and cloud water \), a background correction was not done.](#)

2.3.3 Salinity correction of SML and ULW

SML and ULW samples were adjusted to account for the freezing depression caused by dissolved salts in sea water. First, based on Kreidenweis et al. (2005), the water activity can be calculated by:

$$a_w = \frac{n_{\text{water}}}{n_{\text{water}} + i * n_{\text{solute}}} \quad (3)$$

where the n_{solute} and n_{water} are the number of moles of solute and water in solution, respectively. i is the van't Hoff factor (Pruppacher and Klett, 2010). We assumed sea salt to be mainly sodium chloride, for which the van't Hoff factor is 2. The freezing depression temperature as a function of a_w was taken from Koop and Zobrist (2009). In our study, this was roughly a correction by 2.2 °C.

2.4 Active surface site density

A thorough analysis of particle number size distributions (PNSDs) has been presented in Gong et al. (2019b), and based on these PNSDs we derived the particle surface area size distributions (PASDs) for use in this study (to be seen in the supplement, Fig. S14). This provides an opportunity to determine the temperature-dependent cumulative active surface site density (n_s) for aerosol particles. The n_s is a measure of how well an aerosol acts as a seed surface for ice nucleation. The n_s can be calculated as:

$$n_s = \frac{N_{\text{INP}}(\theta)}{A_{\text{total}}} \quad (4)$$

Where A_{total} is the concentration of the total particle surface area.

For cases where a single type of aerosol, such as one type of mineral dust, is examined in laboratory studies, A_{total} can be the total particle surface area. However, when field experiments are done, using the total particle surface area of the atmospheric aerosol assumes that all particles contribute to INP and have the same n_s , while the vast majority of these particles will not even be an INP. On the other hand, singling out the contribution of separate INP types in the atmospheric aerosol and relying n_s only to them by using their contribution to the total surface area is at least demanding if not often impossible. This has to be kept in mind when interpreting heterogeneous ice nucleation in terms of n_s .

3 Results

3.1 INP in SML and ULW

Based on Eq. 1, the derived N_{INP} in seawater as a function of temperature is shown in Fig. 1, for both SML and ULW. Note that for each sample a separate INP spectrum is shown. Error bars show the 95% confidence interval. For completeness, f_{ice} of all seawater samples is shown in the supplement, Fig. S1 (measured by LINA) and Fig. S2 (measured by INDA). The variation of N_{INP} at any particular temperature is within one order of magnitude. Included in Fig. 1 are previous studies of N_{INP} measured east of Greenland in the Arctic (shown as red box) and east of America in the North Atlantic Ocean (shown as black box) from Wilson et al. (2015).

The concentration range detected for ULW in Wilson et al. (2015) (both in the Arctic and the North Atlantic Ocean) roughly agrees with our data. In Wilson et al. (2015), N_{INP} in the SML in the North Atlantic Ocean is at the lower end of that found in the Arctic. A possible reason for this difference could be the biological activity of the ocean water. Wilson et al. (2015) found that organic material was correlated to N_{INP} in SML, and that N_{INP} per gram of total organic carbon in the Arctic and the North Atlantic Ocean were comparable. A recent study found that the SML at Cape Verde was oligotrophic, which is supported by the low Chlorophyll-a and transparent exopolymer particles concentrations found during the MarParCloud campaign (Robinson et al., 2019). This The low biological activity in the SML around Cape Verde could be the reason why N_{INP} in SML in this study is lower than those reported in Wilson et al. (2015).

To better quantify the enrichment or depletion of N_{INP} in SML to ULW, we derived an enrichment factor (EF). An enrichment might be expected as organic material is known to attach to air bubbles rising to the ocean surface. The EF in SML was calculated by dividing N_{INP} in SML ($N_{\text{INP, SML}}$) by the respective N_{INP} measured in ULW ($N_{\text{INP, ULW}}$), as the below equation shows:

$$\text{EF} = \frac{N_{\text{INP, SML}}}{N_{\text{INP, ULW}}} \quad (5)$$

Enrichment of N_{INP} in the SML is indicated when $\text{EF} > 1$, while depletion is indicated when $\text{EF} < 1$. Fig. 2 shows the EF as a function of the temperature at which N_{INP} was determined in the freezing devices. Both enrichment and depletion were observed, but there is no clear trend of the EF with temperature. Most of the variation seen here is likely caused by measurement uncertainties, which are indicated in Fig. S3 in the supplement. EF varied from 0.36 to 11.40 at -15°C and from 0.36

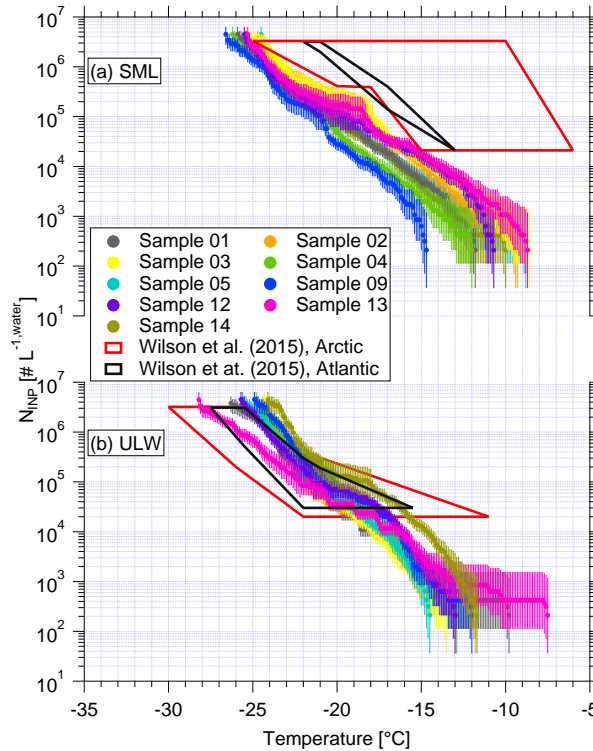


Figure 1. N_{INP} as a function of temperature in SML (a) and ULW (b). Error bars show the 95% confidence interval. Previous field measurements of N_{INP} in seawater by Wilson et al. (2015) are compared, as shown by red and black boxes.

to 7.11 at -20 °C. By comparing T_{10} (the temperature at which 10% of droplets had frozen) for the SML and ULW, Wilson et al. (2015) observed higher enrichment of INPs in SML in both the Arctic and the North Atlantic Ocean. However, Irish et al. (2017) observed both enrichment and depletion of INPs in SML in the Arctic, similar to the observation made in the present study.

- 5 These differences in EF between studies might partially be due to differences in the techniques deployed and different SML thickness in our and the other studies. SML samples were estimated to be about ~ 91.0 μm thick in this study, while for Wilson et al. (2015) those were between 6 to 83 μm . It is interesting to note that we used glass dipping for the samples analyzed in herein, while both glass dipping and a rotating drum sampler were used in Wilson et al. (2015). Previous studies pointed out that rotating drum sampler and the glass dipping method probe different thicknesses of the SML, thus making a direct
- 10 comparison of both SML thickness as well as enrichment factors generally difficult (Agogu  et al., 2004; Aller et al., 2017).

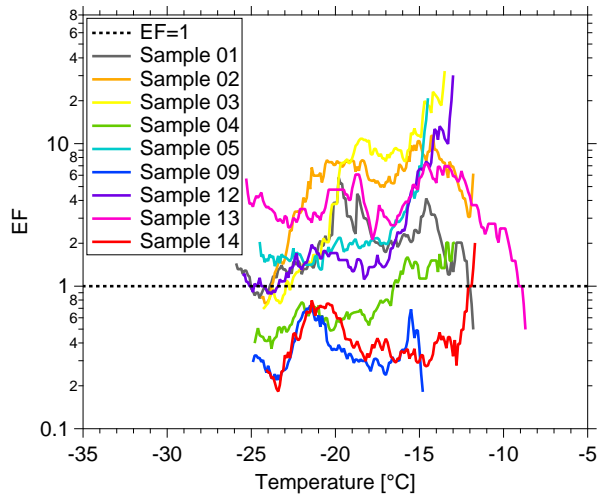


Figure 2. EF as function of [ice nucleation](#) temperature. The EF=1 is shown by dashed line.

3.2 N_{INP} in air

Three different sets of filter samples were collected at CVAO and MV, i.e., CVAO PM_{10} , CVAO PM_1 and MV PM_{10} . In ~~the~~ this section, we will discuss N_{INP} at CVAO for the two different size classes and compare N_{INP} from close to the sea level (CVAO) to that at cloud level (MV).

5 3.2.1 N_{INP} close to sea level

CVAO PM_{10}

N_{INP} as a function of temperature from CVAO PM_{10} filters and CVAO PM_1 filters are shown in Fig. 3(a) and (b). Error bars show the 95% confidence interval. The respective values of f_{ice} are shown in the supplement, Fig. S4 (CVAO PM_{10}) and Fig. S8 (CVAO PM_1), together with the results from the blind filters. The CVAO PM_{10} filter samples were all active at -11.3 °C and the highest freezing temperature was found to be -5.0 °C. Filter samples collected in Cape Verde over the period 2009-2013 for INP measurement were reported by Welti et al. (2018), and they are shown as gray background in Fig. 3(a). The measured N_{INP} in this study is within the N_{INP} range presented by Welti et al. (2018).

N_{INP} at any particular temperature span around 1 order of magnitude below -15 °C, and about 2 orders of magnitude at warmer temperatures. This is consistent with the previous studies from O’Sullivan et al. (2018) and Gong et al. (2019a), who carried out field measurement in northwestern Europe and the eastern Mediterranean, respectively. A few samples (CVAO

1596, CVAO 1641 and CVAO 1643) showed elevated concentrations above 0.01 std L^{-1} at -10°C . Biological particles usually contribute to INPs at this moderate supercooling temperature (Kanji et al., 2017; O’Sullivan et al., 2018).

Biological INPs contain specific ice-nucleating proteins. These proteins are disrupted and denatured by heating which causes them to lose their ice-nucleating ability. However, the inorganic ice-nucleating material, such as dust particles, is insensitive to heat (Wilson et al., 2015; O’Sullivan et al., 2018). Therefore, a commonly used heat treatment was deployed to assess the contribution of biological INPs to the total INPs in this study. Samples CVAO 1596, CVAO 1641 and CVAO 1643 were heated to 95°C for 1 hour and the resulting N_{INP} are shown in Fig. S6. A clear comparison of before and after heating f_{ice} is shown in Fig. S7. A large reduction of more than one order of magnitude in N_{INP} at $T > -15^\circ\text{C}$ was observed in the samples after heating. The reductions in N_{INP} became smaller at colder temperature and were, for example, less than one order of magnitude at $T = -20^\circ\text{C}$. This shows that biological aerosol contributed a large fraction of total INPs in PM_{10} at $T > -20^\circ\text{C}$.

The correlation of N_{INP} at two different temperatures was calculated. The correlation of N_{INP} at different temperatures within one sample was calculated, by comparing each N_{INP} at each temperature to that at each other temperature at which a measurement had been made. That was done separately for each of the samples. For temperature steps of 0.1°C , N_{INP} at every temperature was correlated to that at every other temperature in the measurement range. With increasing difference in temperatures, the variation in N_{INP} at two temperatures become less correlated. As long as the examined temperature difference was less than 2°C , N_{INP} were correlated. But when looking at this in a broader picture, in the temperature region down to $\sim -16.8^\circ\text{C}$, N_{INP} at all temperatures correlated well with that at all other temperatures, with coefficient of determination (R^2) > 0.8 and $p < 0.01$. The same was true for N_{INP} in the temperatures region $< -18.4^\circ\text{C}$. In between these two temperature regimes (between $> -16.8^\circ\text{C}$ and $< -18.4^\circ\text{C}$), the correlation of N_{INP} was clearly lower. Therefore, it might be expected that INPs that are active in these two temperature regimes originated from different sources.

CVAO PM_1 in comparison to CVAO PM_{10}

N_{INP} in PM_1 filters are also determined in this study (as shown in Fig. 3(b)). An initial observation of the data shows that the bulk of the data of N_{INP} for CVAO PM_1 is below that for CVAO PM_{10} . Fig. 4 shows the probability density function (PDF) of N_{INP} in CVAO PM_{10} (black) and CVAO PM_1 (red) at -12°C (a), -15°C (b) and -18°C (c). These temperatures were chosen because for each of them the filters contributes data. Comparing N_{INP} for PM_1 and PM_{10} , a few two key features are evident :

1. Larger particles, i.e., super-micron ones, were more efficient INPs, which is independent of temperature in the examined range.
2. Smaller particles, i.e., submicron ones, exhibited an equal spread of about 1 order of magnitude in N_{INP} for the whole temperature range (see Fig. 3(b)). The elevated N_{INP} at warm temperatures which are seen for CVAO PM_{10} are not observed for CVAO PM_1 .

As for the first feature, we calculated the ratio of N_{INP} in super-micron size range to N_{INP} in PM_{10} during the same time period and found that $83 \pm 22\%$, $67 \pm 18\%$ and $77 \pm 14\%$ (median \pm standard deviation) of INPs had a diameter of $> 1 \mu\text{m}$ at ice activation temperatures of -12 , -15 , and -18°C , respectively. On average, over all temperatures, this INP number fraction for super-micron particles is roughly 70% (shown for a higher temperature resolution in Fig. 4), almost independent of temperature.

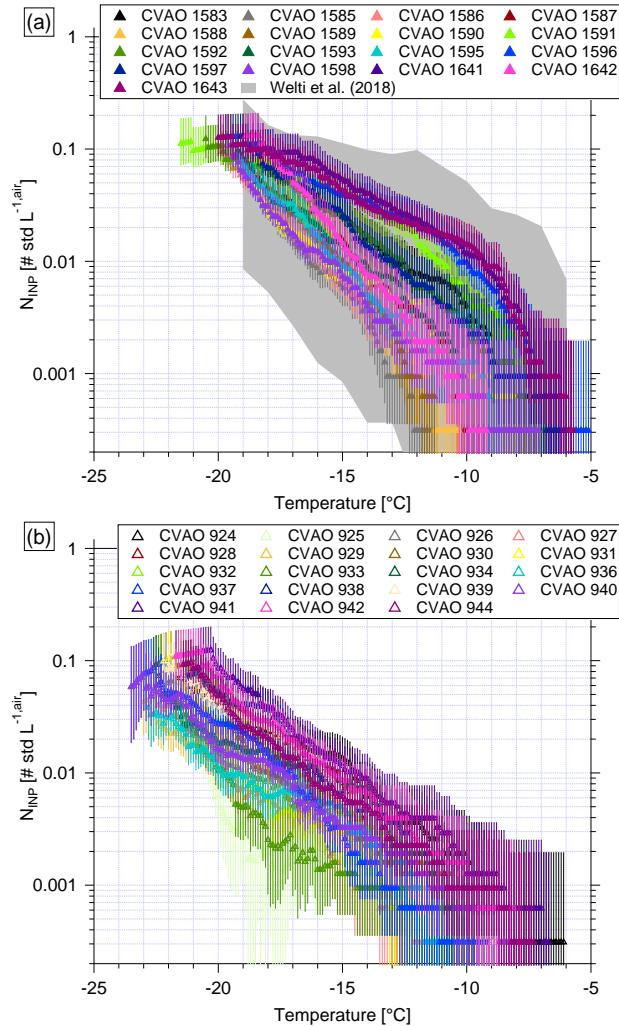


Figure 3. N_{INP} as a function of temperature from CVAO PM₁₀ filters (a) and CVAO PM₁ filters (b). The field measurement of N_{INP} in PM₁₀ by Welts et al. (2018) is shown by gray shadow in Fig. (a). Error bars show the 95% confidence interval.

Mason et al. (2016) and Creamean et al. (2018) also found that the majority of INPs is in the super-micron size range. However, they see even increasing fractions towards higher temperatures. For the present study, as said above, only three of the examined 17 filters showed clearly elevated N_{INP} at high temperatures, so overall such an increase was not observed.

As for the second feature, looking at Fig. 3(b), we found that N_{INP} spread about 1 order of magnitude at any temperature from -12 to -20 $^{\circ}\text{C}$. As outlined above, a few PM₁₀ samples showed elevated concentrations at warm temperatures, showing up as a “bump” in the freezing curves at higher temperatures. This bump at warm temperatures was not observed for the CVAO PM₁ filters. N_{INP} of CVAO 932, CVAO 942 and CVAO 944 (sampled at the same time as CVAO 1596, CVAO 1641 and CVAO 1643) are all below 0.001 std L^{-1} at -10°C . As mentioned above, INP active at comparably high temperatures are generally

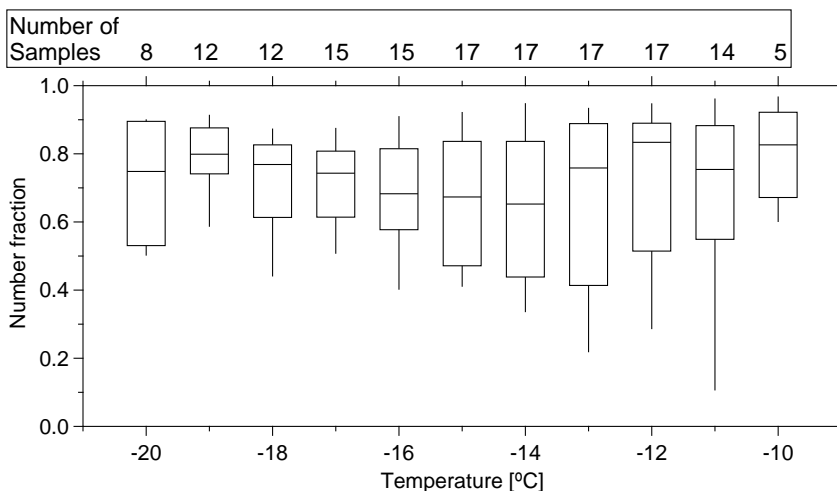


Figure 4. Boxplot of number fraction of INPs in the size range of $>1 \mu\text{m}$ as a function of temperature. [The boxes represent the interquartile range. Whiskers represent 10th to 90th percentile.](#) The number of samples indicated on top of the figure shows how many different samples contributed at the different temperatures.

[assumed were found](#) to be biological in origin [\(e.g., Kanji et al., 2017; O'Sullivan et al., 2018\)](#) in this study, and [our findings suggest the comparison between \$\text{PM}_{10}\$ and \$\text{PM}_1\$ samples show](#) that there are biological INPs in the CVAO PM_{10} samples that are absent in the CVAO PM_1 samples, i.e., that [these likely the detected](#) biological INPs are super-micron in size. [This suggests that these biological INPs might originate from long-range transport, as marine biological INPs were usually reported to be submicron in size \(Wilson et al., 2015; Irish et al., 2017\).](#) The contribution of SSA to INPs will be discussed further in section 3.4.

3.2.2 N_{INP} at cloud level

In the companion paper (Gong et al., 2019b), we discussed PNSD and CCN number concentration (N_{CCN}) at CVAO and MV. We found that particles are mainly well mixed in the marine boundary layer and derived the periods with cloud events, with a time resolution of ~ 30 minutes, at MV. In the present study, N_{INP} in PM_{10} at CVAO and MV are compared. The fraction of time during which there was a cloud event to the total sampling time (cloud time fraction) for each filter is summarized in the supplement, Tab. S4. All of the filters were [more or less](#) affected by cloud events [with a cloud time fraction from 4.17 to 100%](#), with two filters being affected only little (cloud time fraction $< 10\%$), i.e., MV 1602 and MV 1603. When comparing results from these two filters to those from filters sampled at the same time at CVAO (see Fig. 5(a)), we found that N_{INP} are quite similar close to sea level (CVAO) and cloud level (MV). This is in line with what was discussed in the companion paper (Gong et al., 2019b), i.e., the marine boundary is often well mixed at Cape Verde.

Fig. 5(b) compares N_{INP} at CVAO and MV when MV filters were mostly collected during cloud events with cloud time fractions $> 90\%$. During the cloud events, the filters did not collect droplets larger than $10 \mu\text{m}$ because of the inlet cutoff. It is obvious [from Fig. 5](#) that for these cases, N_{INP} at MV is much lower than that at CVAO, implying that particularly INPs that

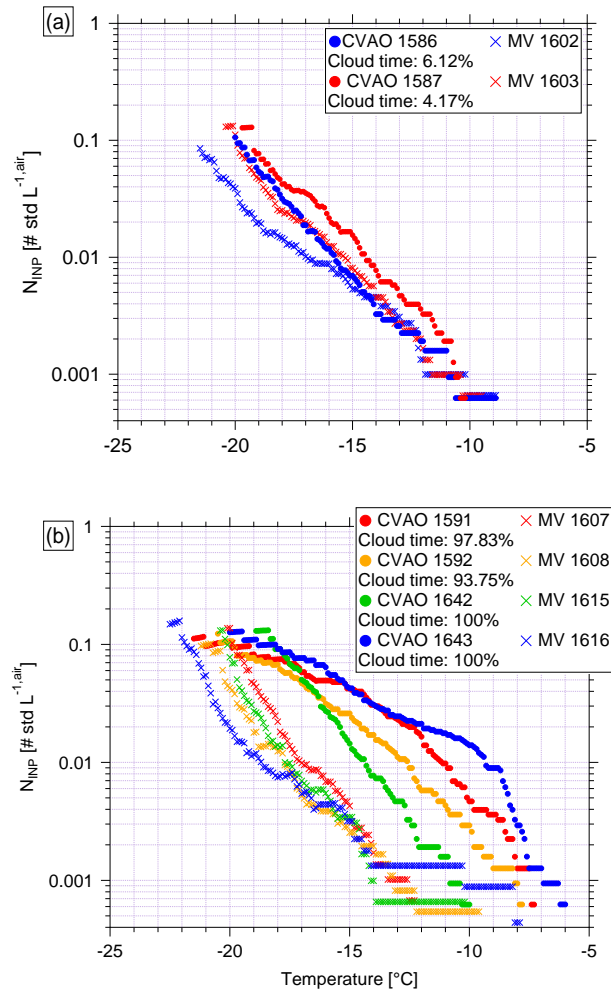


Figure 5. N_{INP} as a function of temperature from CVAO PM₁₀ filters and MV PM₁₀ filters during (a) less (cloud time fraction <10%) cloud effected periods (a) and (b) highly (cloud time fraction >90%) cloud effected periods(b).

were ice active above ~ -17 ° C were activated to cloud droplets to a large degree. But note that even when filters have a cloud time fraction of 100% (MV 1615 and MV 1616), the respective filters still had clearly more INPs on them than the field blind filters (see supplement, Fig S9). This might indicate that either not all INPs are activated to cloud droplets, or, on the other hand, that some INPs were only recently activated to a cloud droplet and the droplet size was smaller than $10 \mu\text{m}$. [These observations are consistent with results by Siebert and Shaw \(2017\) who observed broad cloud droplet size distributions in a size range from \$\sim 5\$ to \$25 \mu\text{m}\$ in shallow cumulus clouds, with the maximum of the distribution still being below \$10 \mu\text{m}\$.](#)

Concerning the super-micron particles of likely biological origin that activated ice already at -10 ° C and above (Fig-4), it is observed that the related corresponding bump is not seen in the corresponding data from MV (MV 1610, MV 1614 and MV

1616 - to be seen in the supplement, Fig. S10). This indicates that these INPs were all activated to cloud droplets during the cloud events, and we will come back to this below.

3.3 INP in cloud water

3.3.1 Main characteristics and N_{INP} in cloud water

- 5 Thirteen cloud water samples were collected during cloud events in this study. Sampling durations varied from 2.5 to 13 hours and volumes varied from 78 to 544 mL. The most abundant inorganic species were Na^+ and Cl^- , followed by SO_4^{2-} , NO_3^- and Mg^{2+} . For example, the mass concentration of Na^+ and Cl^- varied from 5.00 to 46.11 and 9.27 to 70.30 mg L^{-1} , with a mean value of 17.31 and 28.86 mg L^{-1} , respectively. [Somewhat different values which are still roughly in the same range were reported by Gioda et al. \(2009\), who found in Puerto Rico the \$\text{Na}^+\$ and \$\text{Cl}^-\$ concentration in the cloud water varied from](#)
- 10 [3.79 to 15.53 and 5.90 to 23.20 \$\text{mg L}^{-1}\$, with a mean of 10.74 and 15.67 \$\text{mg L}^{-1}\$, respectively, which are comparable to this study.](#) All of the above mentioned parameters are summarized in the supplement, Tab. S5.

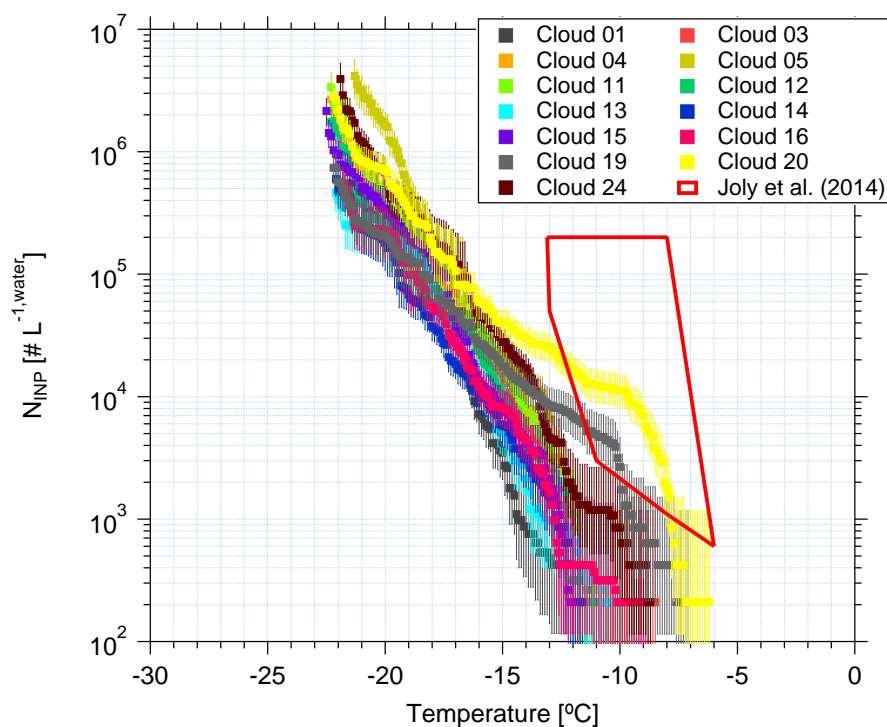


Figure 6. N_{INP} as a function of temperature in cloud water. Error bars show the 95% confidence interval. Previous field measurements of N_{INP} in cloud water by Joly et al. (2014) are compared, as shown by the red box.

Based on Eq. 1, the derived N_{INP} as a function of temperature is shown in Fig. 6. Error bars represent the 95% confidence interval. For completeness, f_{ice} for cloud water is shown in the supplement, Fig. S12 (measured by LINA) and Fig. S13

(measured by INDA). N_{INP} at any particular temperature span less than 1 order of magnitude below $-15\text{ }^{\circ}\text{C}$, while they span 2 orders of magnitude at warmer temperatures. We observed elevated N_{INP} in the cloud water at warm temperatures (above 1000 L^{-1} at $-10\text{ }^{\circ}\text{C}$) particularly for the Cloud 19, Cloud 20 and Cloud 24 samples. Joly et al. (2014) measured the total and biological (i.e., heat-sensitive) INPs between -5 to $-14\text{ }^{\circ}\text{C}$ from the summit of Puy de Dôme (1465 m a.s.l., France), as shown in the red box in Fig. 6. Joly et al. (2014) observed very high concentrations of both biological particles and N_{INP} . Agreement of N_{INP} in cloud water all over the world was not expected, since the sources of INPs are different in different locations.

When highly ice active particles were present for CVAO PM_{10} filters (CVAO 1596, CVAO 1641 and CVAO 1643), they were not observed for MV PM_{10} (MV 1610, MV1614 and MV 1616, which had cloud time fractions of 52, 87 and 100%, respectively), but instead were found in cloud water samples (Cloud 19, Cloud 20 and Cloud 24). This is in line with what was outlined in section 3.2.2 that these highly ice active particles were activated to cloud droplets during cloud events. Periods during which clouds were present at MV, together with the sampling periods of all cloud water samples and selected CVAO PM_{10} filters (those that had higher N_{INP} at warm temperatures, CVAO 1596, CVAO 1641 and CVAO 1643) can be checked in the supplement, Fig. S11.

3.3.2 Connecting INPs in the cloud water with these in the air

In the following, N_{INP} in the cloud water will be compared to that in the air. To be able to do this, we used measured values of N_{CCN} to calculate cloud droplet number concentrations. These, together with an assumption on cloud droplet size (d_{drop}) yields the volume of cloud water per volume of air, given as $F_{\text{cloud_air}}$ in Eq. 6:

$$F_{\text{cloud_air}} = N_{\text{CCN}} * \pi / 6 * d_{\text{drop}}^3 \quad (6)$$

For the calculation, we used N_{CCN} measured at CVAO at a supersaturation of 0.30% (Gong et al., 2019b). N_{CCN} was averaged for the different periods when each cloud water sample was collected. The chosen supersaturation corresponds to a critical diameter of roughly 80 nm, which is at the Hoppel minimum of the respective particle number size distributions (Gong et al., 2019b), indicating that this is indeed the relevant supersaturation occurring in the prevailing clouds. Based on previous studies (Miles et al., 2000; Bréon et al., 2002; Igel and Heever, 2017; Siebert and Shaw, 2017), we assumed that d_{drop} varies between 7 and 20 μm and did separate estimates for these two values and additionally for 15 μm . [The calculation based on this size range of cloud droplets should cover all that can be expected to occur.](#)

Following this approach, $F_{\text{cloud_air}}$ varied from $4.2*10^{-7}$ to $1.1*10^{-6}$, with a median of $8.5*10^{-7}$. [To see how reliable these values are, we also examined the following: assuming all sodium chloride particles were activated to cloud droplets, \$F_{\text{cloud_air}}\$ can be also estimated from the ratio of sodium chloride mass concentration in air to that in cloud water. This ratio varied from \$1.1*10^{-7}\$ to \$4.2*10^{-7}\$, which is at the lower end but still comparable to \$F_{\text{cloud_air}}\$ as we derived it above.](#) Previous studies used the liquid water content (LWC), which is a measure of the mass of the water in a cloud in a specified amount of dry air. Typical ranges for LWC in thicker clouds are between 0.2 and 0.8 g m^{-3} (Rangno and Hobbs, 2005; Petters and Wright, 2015), corresponding to $F_{\text{cloud_air}}$ between $2*10^{-7}$ to $8*10^{-7}$, which [again](#) agreed well with [the above given values derived for this study.](#)

With this $F_{\text{cloud,air}}$, N_{INP} in the respective volume of air can be compared to N_{INP} in this volume of cloud water when assuming that all INPs are CCN, which, based on the super-micron size of most of the INPs alone, is likely. To do so, N_{INP} obtained for cloud water was multiplied by $F_{\text{cloud,air}}$ (for the three different assumptions on d_{drop}) to yield N_{INP} in the air ($N_{\text{INP,air}}$), given in Eq. 7:

$$5 \quad N_{\text{INP,air}} = F_{\text{cloud,air}} * N_{\text{INP,cloud}} \quad (7)$$

Fig. 7 shows the measured N_{INP} in the air as a function of temperature by squares. Derived $N_{\text{INP,air}}$ from cloud water (calculated with a d_{drop} of $15\mu\text{m}$) are shown by triangles. The samples with comparatively high numbers of INPs active at warm temperatures, are shown in different colors. CVAO 1596, CVAO 1641 and CVAO 1643 are shown by green squares (the rest shown by blue squares) and derived $N_{\text{INP,air}}$ from samples collected for Cloud 19, Cloud 20 and Cloud 24 are shown by 10 brown triangles (the rest shown by red triangles). The range of values indicated for $N_{\text{INP,air}}$ was obtained from using 7 and 20 μm cloud droplet size, with 7 μm droplets yielding the lower boundary and 20 μm the upper one.

There is general agreement between measured and derived N_{INP} in air, however, with some variation where the values derived from cloud water samples are somewhat lower. This might be connected to a less than optimal sampling efficiency of the cloud water sampler, which has a 50% collection efficiency at $3.5\mu\text{m}$. Also the spread in the derived values, originating 15 from the different assumed d_{drop} , is rather large. Nevertheless, it is striking that at least within an order of magnitude, based on our comparably simple assumptions, an agreement between concentrations of INP in the air and in cloud water is found.

3.4 INPs originating from sea spray

In the following section, it will briefly be discussed whether SSA contributed noticeably to INPs in the air. Assuming sea salt and INPs to be similarly distributed in both, seawater and air (i.e., assuming that INPs would not be enriched during the 20 production of sea spray), N_{INP} in the air originating from sea spray ($N_{\text{INP}}^{\text{sea spray,air}}$) can be calculated based on Eq. 8:

$$N_{\text{INP}}^{\text{sea spray,air}} = \frac{\text{NaCl}_{\text{mass,air}}}{\text{NaCl}_{\text{mass,seawater}}} * N_{\text{INP}}^{\text{seawater}} \quad (8)$$

where $\text{NaCl}_{\text{mass,air}}$ and $\text{NaCl}_{\text{mass,seawater}}$ are sodium chloride mass concentrations in air and seawater, respectively. $N_{\text{INP}}^{\text{seawater}}$ is the INP number concentration in the seawater (this calculation can be done similarly for both SML and ULW).

$\text{NaCl}_{\text{mass,air}}$ and $\text{NaCl}_{\text{mass,seawater}}$ can be found in the supplement, Tab. S1 and Tab. S2. $\text{NaCl}_{\text{mass,seawater}}$ was very stable, with 25 a median value $\sim 31\text{ g L}^{-1}$. $\text{NaCl}_{\text{mass,air}}$ showed large variability from 3.40 to $17.76\text{ mg L}^{-1}\mu\text{g m}^{-3}$, with a median of $13.08\text{ mg L}^{-1}\mu\text{g m}^{-3}$. Based on Eq. 8, the resulting $N_{\text{INP}}^{\text{sea spray,air}}$ are shown in blue (derived from SML) and green (derived from ULW) in Fig. 8. Irish et al. (2019b) used the same method to get $N_{\text{INP}}^{\text{sea spray,air}}$ in the Arctic (without considering enrichment of INPs in sea salt particles during sea spray generation), as shown by purple (derived from SML) and brown (derived from ULW) boxes in Fig. 8. As discussed in section 3.1, N_{INP} from ULW at Cape Verde are comparable to the Arctic, and the NaCl ratios were 30 close to 10^{-10} in both studies, therefore, $N_{\text{INP}}^{\text{sea spray,air}}$ (derived from ULW) are also comparable. A high enrichment of N_{INP} in SML to ULW was observed in the Arctic (Irish et al., 2019b). Therefore, $N_{\text{INP}}^{\text{sea spray,air}}$ (derived from SML) in the Arctic was also higher than in this study.

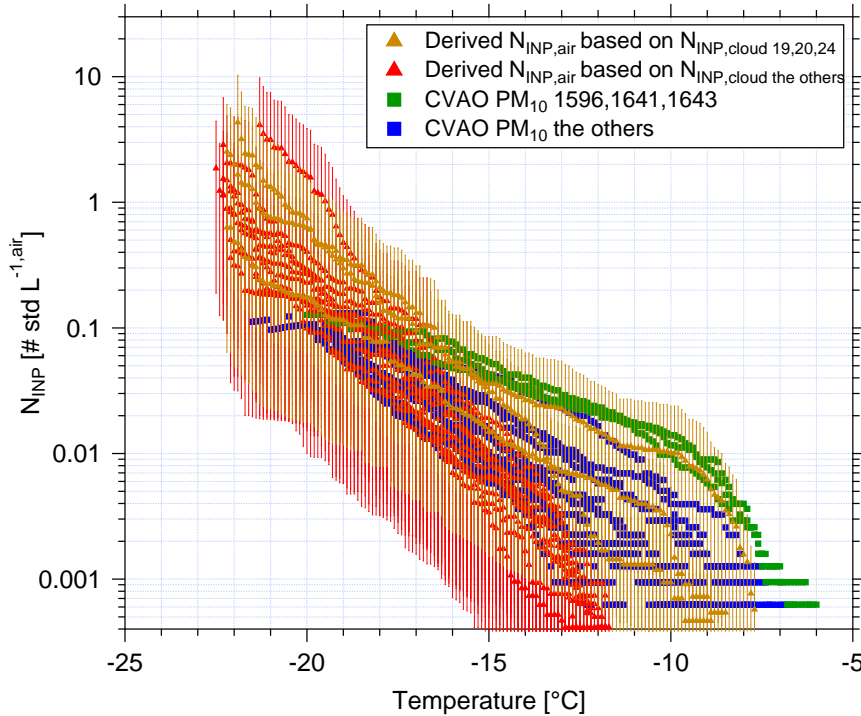


Figure 7. The measured atmospheric N_{INP} as a function of ice nucleation temperature in the air by are shown as squares. The derived $N_{\text{INP,air}}$ based on INP concentrations measured for cloud water are shown by triangles. The samples with highly ice active INPs at warm temperatures, are shown in a different color than the others: CVAO 1596, CVAO 1641 and CVAO 1643 are shown by green squares and derived $N_{\text{INP,air}}$ based on Cloud 19, Cloud 20 and Cloud 24 are shown by brown triangles. The uncertainty range indicated for the derived $N_{\text{INP,air}}$ originate from calculations with 7 and 20 μm cloud droplet size.

Fig. 8 includes N_{INP} from PM_{10} in this study (shown by black triangles). These values are roughly 4 orders of magnitude above our $N_{\text{INP}}^{\text{sea spray,air}}$. But Fig. 8 also shows airborne N_{INP} as derived for the Southern Ocean (McCluskey et al., 2018a) and the Northeast Atlantic (only clean sector, McCluskey et al., 2018b), which are all above our $N_{\text{INP}}^{\text{sea spray,air}}$. As mentioned above, we did not consider a possible enrichment of INPs in SSA compared to the SML or ULW samples. Previous studies

5 found an enrichment of organic carbon in submicron sea spray particles of about 10^4 to 10^5 (Keene et al., 2007; van Pinxteren et al., 2017), and this value decreased to 10^2 for super-micron particles (Keene et al., 2007; Quinn et al., 2015). It is not clear if INPs are included in the organic carbon for which the enrichment was observed. Also, the INPs we detected in this

10 study were mostly in the super-micron size range. If we increased $N_{\text{INP}}^{\text{sea spray,air}}$ by about 2 orders of magnitude in agreement to the enrichment observed for super-micron organic carbon, the resulting $N_{\text{INP}}^{\text{sea spray,air}}$ becomes comparable to sea spray INPs measured in the Southern Ocean (McCluskey et al., 2018a) and the Northeast Atlantic (McCluskey et al., 2018b). But even when considering such an enrichment of INPs, INPs originating from sea spray would only explain a small fraction of all INPs contributing to the measured airborne N_{INP} in the air at Cape Verde.

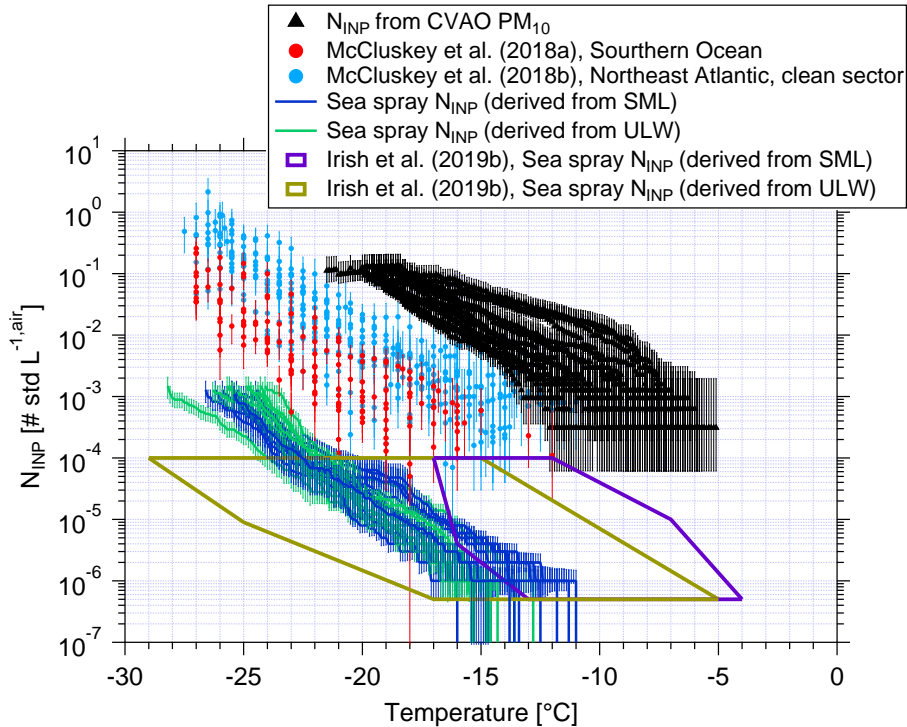


Figure 8. Atmospheric N_{INP} are shown as a function of temperature from PM_{10} filters (black triangles), and error bars show together with error bars showing the 95% confidence interval. N_{INP} as a function of temperature from McCluskey et al. (2018a, b) are shown by red and light blue dots, respectively. Error bars show the 95% confidence interval. $N_{\text{INP}}^{\text{sea spray,air}}$ from this study are shown by blue (derived from SML) and green lines (derived from ULW). $N_{\text{INP}}^{\text{sea spray,air}}$ from Irish et al. (2019b) are shown by purple (derived from SML) and brown (derived from ULW) boxes.

4 Discussion

N_{INP} close to sea and cloud level height were compared. One major point of interest is to know whether ground-based measurements can be used to infer aerosol properties at the cloud level. In this study, we found that N_{INP} are quite similar close to sea level (CVAO) and cloud level (MV) during non-cloud events. But it should still be noted that we only have a small number of filter samples representing non-cloud events in this study. During the observed cloud events, most INPs at MV are activated to cloud droplets. The above findings are in line with what was discussed in the companion paper (Gong et al., 2019b), i.e., (1) the marine boundary is often well mixed at Cape Verde and PNSDs and N_{CCN} are similar close to both sea and cloud level; (2) during cloud events, larger particles are activated to cloud droplets.

Most INPs are in the super-micron size range at Cape Verde. We found that about 70% of INPs had a diameter of $>1 \mu\text{m}$ at ice activation temperatures between -10 and -20 °C. Mason et al. (2016) and Creamean et al. (2018) also found that the majority of INPs is in the super-micron size range in the Arctic, in agreement with the results we obtained here.

Above we derived that N_{INP} contributed from SSA only accounted for a minor fraction of total N_{INP} in the air, as well as in the cloud water at Cape Verde. This still holds even when considering a possible enrichment of INPs in SSA up to 10^2 , which is an enrichment as given in literature for super-micron organic particles (Keene et al., 2007; Quinn et al., 2015). ~~It can similarly be seen when considering that it has been described in literature that mineral dust is associated with a factor of 1000 higher ice surface site density (a measure to describe the ice activity per particle surface area), compared to SSA at temperatures from -12 to -35 °C~~ On the other hand, mineral dust is associated with a factor of 1000 higher ice surface site density (a measure to describe the ice activity per particle surface area), compared to SSA (Niemand et al., 2012; DeMott et al., 2016; McCluskey et al., 2018a). In our study, the super-micron particles that make up a large fraction of the INPs we observed were mainly mineral dust, as described in the accompanying study (Gong et al., 2019b). The comparably high ice activity of super-micron mineral dust and the presence of mainly dust particles in the super-micron size range in our study again supports that indeed most INPs observed in this study were not from sea spray. This is in line with results from Si et al. (2018) and Irish et al. (2019a), both done in the Arctic, where it was also concluded that SSA only contributed little to the INP population. The commonality of these two studies from the Arctic and the present study is that land was still close enough so that terrestrial sources can have contributed to the observed INPs.

While the above arguments suggest that INPs in our study were mostly mineral dust particles, there were also some measurements with comparably high INP concentrations at temperatures of -10 °C and above. Although it cannot be ruled out that desert dust particles might be ice active at such high temperatures, by examining the reaction of some highly ice active samples to heating, described in Sec. 3.2.1, we found that the most highly ice active INPs on these samples were biological particles. It is an open question where these ~~highly ice active~~ biological INPs originated. ~~Such high ice activity is typically associated with biological particles.~~ The times during which these highly ice active INPs were observed were times when air masses came from Southern Europe, traveling along the African coast and meanwhile crossing over the region of the Canary Islands. Therefore, for these specific samples, a contribution of INPs from these land sources might be assumed.

Finally, In the following, we will compare n_s derived from our data with that from literature. In Fig. 9, we show the surface site density derived for ~~our data~~ N_{INP} from CVAO PM_{10} filters (as shown by black boxes) following Niemand et al. (2012) (details on the surface area are given in the supplement, Fig. S14), together with parameterizations for n_s given by Niemand et al. (2012), Ullrich et al. (2017) and McCluskey et al. (2018b), and the measured n_s given by DeMott et al. (2016) and Price et al. (2018). Niemand et al. (2012) derived n_s from a laboratory study, based on aerosol consisting purely of desert dust particles. It is therefore reasonable that these mineral dust related n_s values are the largest values shown in Fig. 9, as they are purely related to the mineral dust surface area of an aerosol. All other values shown in Fig. 9 were derived for atmospheric measurements, and the surface area used to derive n_s was always based on measured particle number concentrations. Price et al. (2018) carried out airborne measurements in dust laden air over the tropical Atlantic. Parameterizations from McCluskey et al. (2018b) were done for pristine SSA over the Northeast Atlantic and both laboratory and atmospheric measurements of SSA were the base for the n_s parameterization given in DeMott et al. (2016). These available n_s parameterizations from previous literature may not be representative for Cape Verde, but we will still compare with them here. n_s derived for our study coincides with the upper range of parameterizations that are otherwise reported for SSA but are clearly lower than values reported for atmospheric desert dust aerosol. This is striking since, as discussed above, INPs observed in this study most likely do not originate from

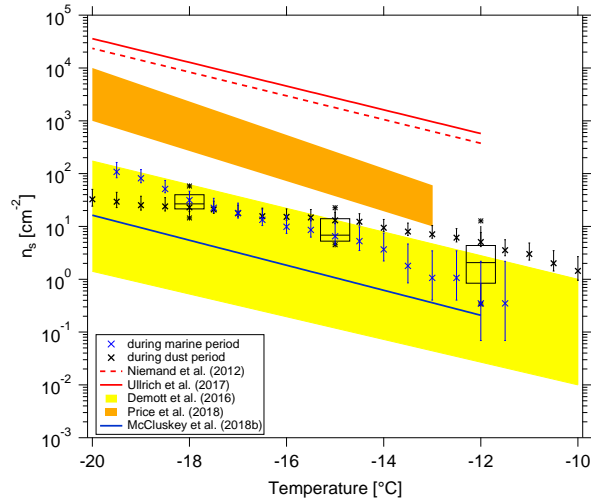


Figure 9. n_s as a function of temperature in this study is shown by black boxes. The boxes represent the interquartile range. Whiskers represent 10th to 90th percentile. Data not included between the whiskers are plotted as an outlier with a star. Two n_s parameterizations (Niemand et al., 2012; Ullrich et al., 2017) for pure desert dust are shown in dashed and solid red lines, respectively. n_s parameterizations from McCluskey et al. (2018b) for pristine SSA over the Northeast Atlantic are shown as a solid blue line. We also compare to recent data from airborne measurement in a dust layer by Price et al. (2018) in brown shadow and from nascent laboratory generated and ambient SSA by DeMott et al. (2016) in yellow shadow, respectively. n_s during the most clean marine (CVAO 1585) and most dusty (CVAO 1591) periods are shown as blue and black crosses, respectively.

sea spray, but are dominated by super-micron dust and/or biological particles. ~~This raises the question if and how n_s should be used to parameterize atmospheric INP measurements, which, however, is a question far too prominent to be answered in this study.~~

CVAO is a place where marine and dust particles strongly intersect, and both particle types contribute to the surface area. In the companion paper, we have classified the aerosol at CVAO into four different types. Here, in addition to looking at average values as presented above, we selected the most clean marine (CVAO 1585) and most dusty (CVAO 1591) samples for a separate calculation of n_s and added the results to Fig. 9. The n_s is clearly higher for the sample collected during the dusty period than during the marine period at higher temperatures (roughly > -16 °C). However, at temperatures below -18 °C it is the other way around. In general, results for these vastly different cases are both still close to the upper limit of the parameterizations reported for SSA.

10 These comparisons to literature raise the question if and how n_s should be used to parameterize atmospheric INP measurements, which, however, is a question far too prominent to be answered in this study. In general, it is still an open issue to which extent N_{INP} can be parameterized, based on one or a few parameters, to reliably describe N_{INP} for different locations around the globe. It might prove necessary to develop separate parameterizations for different locations or air masses, as it was already started for parameterizations based on particle number concentrations (see e.g., DeMott et al. (2010); Tobo et al. (2013); DeMott et al. (201

5 Summary and conclusions

The MarParCloud campaign took place in September and October 2018 on the island of Cape Verde to investigate aerosols prevailing in the Atlantic Ocean. In addition to a thorough analysis of the atmospheric aerosol particles and CCN in a companion paper (Gong et al., 2019b), samples collected for INPs analysis in this study include: sea surface microlayer (SML) and underlying water (ULW) from the ocean upwind of the island; quartz fiber filter samples of atmospheric aerosol, collected on a tower installed at the island shore and on a 744 m high mountaintop, as well as cloud water collected during cloud events on the mountaintop. N_{INP} were measured offline with two types of freezing devices, yielding results in the temperature range from roughly -5 to -25 °C.

Both enrichment and depletion of N_{INP} in SML to ULW were observed. The enrichment factors (EF) varied from 0.36 to 11.40 and from 0.36 to 7.11 at -15 and -20 °C, respectively, and were generally independent of the freezing temperature at which N_{INP} was determined in the freezing devices.

The measured N_{INP} in this study is consistent with the previous study of Welts et al. (2018), who characterized INPs sampled at CVAO over a time period of 4 years. A few CVAO PM_{10} filter samples (CVAO 1596, CVAO 1641 and CVAO 1643) showed elevated N_{INP} at high temperatures, e.g., above 0.01 std L^{-1} at -10 °C. These elevated values disappeared after heating the samples at 95 °C for 1 hour. Therefore, biological particles appear to contribute to INPs at these moderate supercooling temperatures. Biological particles usually contributed the INPs at this moderate supercooling temperatures (Kanji et al., 2017; O'Sullivan et al., 2018).

About $83 \pm 22\%$, $67 \pm 18\%$ and $77 \pm 14\%$ (median \pm standard deviation) of INPs had a diameter $>1 \mu\text{m}$ at ice activation temperatures of -12 , -15 , and -18 °C, respectively, and over the whole examined temperature range, on average roughly 70% of all INPs were super-micron, independent of the temperature. The highly ice active INPs were not found on the CVAO PM_{10} filters, which suggests that most of these likely biological INPs are in the super-micron size range.

N_{INP} were quite similar at CVAO and MV during non-cloud events. As MV was in clouds most of the time, only two filters could be collected on MV that were affected by cloud for less than 10% of the sampling time. For these, N_{INP} were similar at CVAO and MV. During cloud events, most INPs at MV were activated into cloud droplets. These findings aligned very well with the companion paper, i.e., during non-cloud events, PNSDs and N_{CCN} are similar at CVAO and MV, while during cloud events, larger particles at MV are activated to clouds (see Fig. 8 in the companion paper). When highly ice active particles were present on CVAO PM_{10} filters, they were not observed on MV PM_{10} filters, but were instead observed in the respective cloud water samples. This shows that these INPs are activated into cloud droplets during cloud events.

By comparing N_{INP} derived for the different examined samples, it was found that values in air and in cloud water agreed well. We also compared atmospheric N_{INP} to those in SML and ULW, based on the ratio of sodium chloride concentrations measured for the atmosphere and for SML and ULW. From that we concluded that marine INPs from sea spray can only explain a small fraction of all atmospheric INPs at Cape Verde, unless there would be an enrichment of INPs from SML to the atmosphere by at least a factor of 10^4 . Such an enrichment, however, is higher than anything observed for organic compounds in super-micron particles so far. Generally low INP concentrations are found over remote oceanic regions, compared to locations closer to land masses, implying that the ocean is a weak source of INPs, compared to land. Summarizing, it can be assumed

that most atmospheric INPs detected in the present study were mainly contributed by the dust particles at cold temperatures possibly with few contributions from biological particles at warmer temperatures.

Data availability. The data are available through the World Data Center PANGAEA (<https://www.pangaea.de/>) in the near future. A link to the data can be found under this paper's assets tab on ACP's journal website.

- 5 *Author contributions.* X. Gong wrote the manuscript with contributions from H. Wex and M. van Pinxteren. C. Stolle, N. Triesch and B. Robinson collected ocean water samples. X. Gong, M. van Pinxteren and N. Triesch collected filter samples. K. W. Fomba collected cloud water samples. X. Gong and J. Lubitz performed INP measurements. X. Gong performed data evaluation. X. Gong, H. Wex and F. Stratmann discussed the results and further analysis after the campaign. All co-authors proofread and commented the manuscript.

Competing interests. The authors declare that they have no conflict of interests.

- 10 *Acknowledgements.* The works were carried out in the framework of the MarParCloud project. The authors acknowledge the Leibniz Association SAW funding for the project "Marine biological production, organic aerosol particles and marine clouds: a Process Chain (MarPar-Cloud)", SAW-2016-TROPOS-2.

References

- Agogu , H., Casamayor, E. O., Joux, F., Obernosterer, I., Dupuy, C., Lantoin , F., Catala, P., Weinbauer, M. G., Reinthaler, T., Herndl, G. J., and Lebaron, P.: Comparison of samplers for the biological characterization of the sea surface microlayer, *Limnology and Oceanography: Methods*, 2, 213–225, <https://doi.org/10.4319/lom.2004.2.213>, <https://aslopubs.onlinelibrary.wiley.com/doi/abs/10.4319/lom.2004.2.213>, 5 2004.
- Agresti, A. and Coull, B. A.: Approximate is Better than “Exact” for Interval Estimation of Binomial Proportions, *The American Statistician*, 52, 119–126, <https://doi.org/10.1080/00031305.1998.10480550>, <https://doi.org/10.1080/00031305.1998.10480550>, 1998.
- Aller, J. Y., Radway, J. C., Kilhau, W. P., Bothe, D. W., Wilson, T. W., Vaillancourt, R. D., Quinn, P. K., Coffman, D. J., Murray, B. J., and Knopf, D. A.: Size-resolved characterization of the polysaccharidic and proteinaceous components of sea spray aerosol, *Atmospheric Environment*, 154, 331–347, <https://doi.org/https://doi.org/10.1016/j.atmosenv.2017.01.053>, <http://www.sciencedirect.com/science/article/pii/S1352231017300699>, 2017.
- Ansmann, A., Tesche, M., Althausen, D., M ller, D., Seifert, P., Freudenthaler, V., Heese, B., Wiegner, M., Pisani, G., Knippertz, P., and Dubovik, O.: Influence of Saharan dust on cloud glaciation in southern Morocco during the Saharan Mineral Dust Experiment, *Journal of Geophysical Research: Atmospheres*, 113, <https://doi.org/10.1029/2007jd008785>, <https://agupubs.onlinelibrary.wiley.com/doi/abs/10.1029/2007JD008785>, 15 2008.
- Atkinson, J. D., Murray, B. J., Woodhouse, M. T., Whale, T. F., Baustian, K. J., Carslaw, K. S., Dobbie, S., O’Sullivan, D., and Malkin, T. L.: The importance of feldspar for ice nucleation by mineral dust in mixed-phase clouds, *Nature*, 498, 355, <https://doi.org/10.1038/nature12278> <https://www.nature.com/articles/nature12278#supplementary-information>, <https://doi.org/10.1038/nature12278>, 2013.
- 20 Augustin-Bauditz, S., Wex, H., Kanter, S., Ebert, M., Niedermeier, D., Stolz, F., Prager, A., and Stratmann, F.: The immersion mode ice nucleation behavior of mineral dusts: A comparison of different pure and surface modified dusts, *Geophysical Research Letters*, 41, 7375–7382, <https://doi.org/10.1002/2014gl061317>, <https://agupubs.onlinelibrary.wiley.com/doi/abs/10.1002/2014GL061317>, 2014.
- Bigg, E. K.: Ice Nucleus Concentrations in Remote Areas, *Journal of the Atmospheric Sciences*, 30, 1153–1157, [https://doi.org/doi:10.1175/1520-0469\(1973\)030<1153:INCIRA>2.0.CO;2](https://doi.org/doi:10.1175/1520-0469(1973)030<1153:INCIRA>2.0.CO;2), <http://journals.ametsoc.org/doi/abs/10.1175/1520-0469%281973%29030%3C1153%3AINCIRA%3E2.0.CO%3B2>, 1973.
- Boose, Y., Welti, A., Atkinson, J., Ramelli, F., Danielczok, A., Bingemer, H. G., Pl tze, M., Sierau, B., Kanji, Z. A., and Lohmann, U.: Heterogeneous ice nucleation on dust particles sourced from nine deserts worldwide – Part 1: Immersion freezing, *Atmospheric Chemistry and Physics*, 16, 15 075–15 095, <https://doi.org/10.5194/acp-16-15075-2016>, <https://www.atmos-chem-phys.net/16/15075/2016/>, 2016.
- Br on, F.-M., Tanr , D., and Generoso, S.: Aerosol Effect on Cloud Droplet Size Monitored from Satellite, *Science*, 295, 834–838, <https://doi.org/10.1126/science.1066434>, <https://science.sciencemag.org/content/sci/295/5556/834.full.pdf>, 2002.
- 30 Brier, G. W. and Kline, D. B.: Ocean Water as a Source of Ice Nuclei, *Science*, 130, 717–718, <https://doi.org/10.1126/science.130.3377.717>, 1959.
- Budke, C. and Koop, T.: BINARY: an optical freezing array for assessing temperature and time dependence of heterogeneous ice nucleation, *Atmos. Meas. Tech.*, 8, 689–703, <https://doi.org/10.5194/amt-8-689-2015>, <http://www.atmos-meas-tech.net/8/689/2015/>, 2015.
- 35 Burrows, S. M., Hoose, C., P schl, U., and Lawrence, M. G.: Ice nuclei in marine air: biogenic particles or dust?, *Atmos. Chem. Phys.*, 13, 245–267, <https://doi.org/10.5194/acp-13-245-2013>, <https://www.atmos-chem-phys.net/13/245/2013/>, 2013.

- Chen, J., Wu, Z., Augustin-Bauditz, S., Grawe, S., Hartmann, M., Pei, X., Liu, Z., Ji, D., and Wex, H.: Ice-nucleating particle concentrations unaffected by urban air pollution in Beijing, China, *Atmos. Chem. Phys.*, 18, 3523–3539, <https://doi.org/10.5194/acp-18-3523-2018>, <https://www.atmos-chem-phys.net/18/3523/2018/>, 2018.
- Chou, C., Stetzer, O., Weingartner, E., Jurányi, Z., Kanji, Z. A., and Lohmann, U.: Ice nuclei properties within a Saharan dust event at the Jungfrauoch in the Swiss Alps, *Atmos. Chem. Phys.*, 11, 4725–4738, <https://doi.org/10.5194/acp-11-4725-2011>, <http://www.atmos-chem-phys.net/11/4725/2011/>, 2011.
- Conen, F., Henne, S., Morris, C. E., and Alewell, C.: Atmospheric ice nucleators active $\geq -12^{\circ}\text{C}$ can be quantified on PM_{10} filters, *Atmos. Meas. Tech.*, 5, 321–327, <https://doi.org/10.5194/amt-5-321-2012>, <https://www.atmos-meas-tech.net/5/321/2012/>, 2012.
- Conen, F., Eckhardt, S., Gundersen, H., Stohl, A., and Yttri, K. E.: Rainfall drives atmospheric ice-nucleating particles in the coastal climate of southern Norway, *Atmos. Chem. Phys.*, 17, 11 065–11 073, <https://doi.org/10.5194/acp-17-11065-2017>, <https://www.atmos-chem-phys.net/17/11065/2017/>, 2017.
- Creamean, J. M., Kirpes, R. M., Pratt, K. A., Spada, N. J., Maahn, M., de Boer, G., Schnell, R. C., and China, S.: Marine and terrestrial influences on ice nucleating particles during continuous springtime measurements in an Arctic oilfield location, *Atmos. Chem. Phys.*, 18, 18 023–18 042, <https://doi.org/10.5194/acp-18-18023-2018>, <https://www.atmos-chem-phys.net/18/18023/2018/>, 2018.
- DeMott, P. J., Sassen, K., Poellot, M. R., Baumgardner, D., Rogers, D. C., Brooks, S. D., Prenni, A. J., and Kreidenweis, S. M.: African dust aerosols as atmospheric ice nuclei, *Geophysical Research Letters*, 30, n/a–n/a, <https://doi.org/10.1029/2003GL017410>, <http://dx.doi.org/10.1029/2003GL017410>, 2003.
- DeMott, P. J., Prenni, A. J., Liu, X., Kreidenweis, S. M., Petters, M. D., Twohy, C. H., Richardson, M. S., Eidhammer, T., and Rogers, D. C.: Predicting global atmospheric ice nuclei distributions and their impacts on climate, *Proceedings of the National Academy of Sciences*, 107, 11 217–11 222, <https://doi.org/10.1073/pnas.0910818107>, <http://www.pnas.org/content/107/25/11217.abstract>, 2010.
- DeMott, P. J., Prenni, A. J., McMeeking, G. R., Sullivan, R. C., Petters, M. D., Tobo, Y., Niemand, M., Möhler, O., Snider, J. R., Wang, Z., and Kreidenweis, S. M.: Integrating laboratory and field data to quantify the immersion freezing ice nucleation activity of mineral dust particles, *Atmos. Chem. Phys.*, 15, 393–409, <https://doi.org/10.5194/acp-15-393-2015>, <https://www.atmos-chem-phys.net/15/393/2015/>, 2015.
- DeMott, P. J., Hill, T. C. J., McCluskey, C. S., Prather, K. A., Collins, D. B., Sullivan, R. C., Ruppel, M. J., Mason, R. H., Irish, V. E., Lee, T., Hwang, C. Y., Rhee, T. S., Snider, J. R., McMeeking, G. R., Dhaniyala, S., Lewis, E. R., Wentzell, J. J. B., Abbatt, J., Lee, C., Sultana, C. M., Ault, A. P., Axson, J. L., Diaz Martinez, M., Venero, I., Santos-Figueroa, G., Stokes, M. D., Deane, G. B., Mayol-Bracero, O. L., Grassian, V. H., Bertram, T. H., Bertram, A. K., Moffett, B. F., and Franc, G. D.: Sea spray aerosol as a unique source of ice nucleating particles, *Proceedings of the National Academy of Sciences*, 113, 5797–5803, <https://doi.org/10.1073/pnas.1514034112>, <http://www.pnas.org/content/113/21/5797.abstract>, 2016.
- Demoz, B. B., Collett, J. L., and Daube, B. C.: On the Caltech Active Strand Cloudwater Collectors, *Atmospheric Research*, 41, 47–62, [https://doi.org/https://doi.org/10.1016/0169-8095\(95\)00044-5](https://doi.org/https://doi.org/10.1016/0169-8095(95)00044-5), <http://www.sciencedirect.com/science/article/pii/0169809595000445>, 1996.
- Gioda, A., Mayol-Bracero, O. L., Morales-García, F., Collett, J., Decesari, S., Emblico, L., Facchini, M. C., Morales-De Jesús, R. J., Mertes, S., Borrmann, S., Walter, S., and Schneider, J.: Chemical Composition of Cloud Water in the Puerto Rican Tropical Trade Wind Cumuli, *Water, Air, and Soil Pollution*, 200, 3–14, <https://doi.org/10.1007/s11270-008-9888-4>, <https://doi.org/10.1007/s11270-008-9888-4>, 2009.

- Gong, X., Wex, H., Müller, T., Wiedensohler, A., Höhler, K., Kandler, K., Ma, N., Dietel, B., Schiebel, T., Möhler, O., and Stratmann, F.: Characterization of aerosol properties at Cyprus, focusing on cloud condensation nuclei and ice nucleating particles, *Atmos. Chem. Phys. Discuss.*, 2019, 1–34, <https://doi.org/10.5194/acp-2019-198>, <https://www.atmos-chem-phys-discuss.net/acp-2019-198/>, 2019a.
- Gong, X., Wex, H., Voigtländer, J., Fomba, K. W., Weinhold, K., van Pinxteren, M., Henning, S., Müller, T., Herrmann, H., and Stratmann, F.: Characterization of aerosol particles at Cape Verde close to sea and cloud level heights – Part 1: particle number size distribution, cloud condensation nuclei and their origins, *Atmos. Chem. Phys. Discuss.*, 2019, 1–31, <https://doi.org/10.5194/acp-2019-585>, <https://www.atmos-chem-phys-discuss.net/acp-2019-585/>, 2019b.
- Hartmann, M., Blunier, T., Brügger, S., Schmale, J., Schwikowski, M., Vogel, A., Wex, H., and Stratmann, F.: Variation of Ice Nucleating Particles in the European Arctic Over the Last Centuries, *Geophysical Research Letters*, 0, <https://doi.org/10.1029/2019gl082311>, <https://agupubs.onlinelibrary.wiley.com/doi/abs/10.1029/2019GL082311>, 2019.
- Harvey, G. W. and Burzell, L. A.: A simple microlayer method for small samples, *Limnology and Oceanography*, 17, 156–157, <https://doi.org/doi:10.4319/lo.1972.17.1.0156>, <https://aslopubs.onlinelibrary.wiley.com/doi/abs/10.4319/lo.1972.17.1.0156>, 1972.
- Hoose, C. and Möhler, O.: Heterogeneous ice nucleation on atmospheric aerosols: a review of results from laboratory experiments, *Atmos. Chem. Phys.*, 12, 9817–9854, <https://doi.org/10.5194/acp-12-9817-2012>, <http://www.atmos-chem-phys.net/12/9817/2012/>, 2012.
- Huffman, J. A., Prenni, A. J., DeMott, P. J., Pöhlker, C., Mason, R. H., Robinson, N. H., Fröhlich-Nowoisky, J., Tobo, Y., Després, V. R., Garcia, E., Gochis, D. J., Harris, E., Müller-Germann, I., Ruzene, C., Schmer, B., Sinha, B., Day, D. A., Andreae, M. O., Jimenez, J. L., Gallagher, M., Kreidenweis, S. M., Bertram, A. K., and Pöschl, U.: High concentrations of biological aerosol particles and ice nuclei during and after rain, *Atmos. Chem. Phys.*, 13, 6151–6164, <https://doi.org/10.5194/acp-13-6151-2013>, <https://www.atmos-chem-phys.net/13/6151/2013/>, 2013.
- Igel, A. L. and Heever, S. C. v. d.: The Importance of the Shape of Cloud Droplet Size Distributions in Shallow Cumulus Clouds. Part II: Bulk Microphysics Simulations, *Journal of the Atmospheric Sciences*, 74, 259–273, <https://doi.org/10.1175/jas-d-15-0383.1>, <https://journals.ametsoc.org/doi/abs/10.1175/JAS-D-15-0383.1>, 2017.
- Irish, V. E., Elizondo, P., Chen, J., Chou, C., Charette, J., Lizotte, M., Ladino, L. A., Wilson, T. W., Gosselin, M., Murray, B. J., Polishchuk, E., Abbatt, J. P. D., Miller, L. A., and Bertram, A. K.: Ice-nucleating particles in Canadian Arctic sea-surface microlayer and bulk seawater, *Atmos. Chem. Phys.*, 17, 10 583–10 595, <https://doi.org/10.5194/acp-17-10583-2017>, <https://www.atmos-chem-phys.net/17/10583/2017/>, 2017.
- Irish, V. E., Hanna, S. J., Willis, M. D., China, S., Thomas, J. L., Wentzell, J. J. B., Cirisan, A., Si, M., Leitch, W. R., Murphy, J. G., Abbatt, J. P. D., Laskin, A., Girard, E., and Bertram, A. K.: Ice nucleating particles in the marine boundary layer in the Canadian Arctic during summer 2014, *Atmos. Chem. Phys.*, 19, 1027–1039, <https://doi.org/10.5194/acp-19-1027-2019>, <https://www.atmos-chem-phys.net/19/1027/2019/>, 2019a.
- Irish, V. E., Hanna, S. J., Xi, Y., Boyer, M., Polishchuk, E., Ahmed, M., Chen, J., Abbatt, J. P. D., Gosselin, M., Chang, R., Miller, L. A., and Bertram, A. K.: Revisiting properties and concentrations of ice-nucleating particles in the sea surface microlayer and bulk seawater in the Canadian Arctic during summer, *Atmos. Chem. Phys.*, 19, 7775–7787, <https://doi.org/10.5194/acp-19-7775-2019>, <https://www.atmos-chem-phys.net/19/7775/2019/>, 2019b.
- Joly, M., Amato, P., Deguillaume, L., Monier, M., Hoose, C., and Delort, A. M.: Quantification of ice nuclei active at near 0 °C temperatures in low-altitude clouds at the Puy de Dôme atmospheric station, *Atmos. Chem. Phys.*, 14, 8185–8195, <https://doi.org/10.5194/acp-14-8185-2014>, <https://www.atmos-chem-phys.net/14/8185/2014/>, 2014.

- Kanji, Z. A., Ladino, L. A., Wex, H., Boose, Y., Burkert-Kohn, M., Cziczo, D. J., and Krämer, M.: Overview of Ice Nucleating Particles, *Meteorological Monographs*, 58, 1.1–1.33, <https://doi.org/10.1175/amsmonographs-d-16-0006.1>, <https://journals.ametsoc.org/doi/abs/10.1175/AMSMONOGRAPHIS-D-16-0006.1>, 2017.
- Keene, W. C., Maring, H., Maben, J. R., Kieber, D. J., Pszenny, A. A. P., Dahl, E. E., Izaguirre, M. A., Davis, A. J., Long, M. S., Zhou, X., Smoydzin, L., and Sander, R.: Chemical and physical characteristics of nascent aerosols produced by bursting bubbles at a model air-sea interface, *Journal of Geophysical Research: Atmospheres*, 112, <https://doi.org/10.1029/2007jd008464>, <https://agupubs.onlinelibrary.wiley.com/doi/abs/10.1029/2007JD008464>, 2007.
- Koop, T. and Zobrist, B.: Parameterizations for ice nucleation in biological and atmospheric systems, *Physical Chemistry Chemical Physics*, 11, 10 839–10 850, <https://doi.org/10.1039/B914289D>, <http://dx.doi.org/10.1039/B914289D>, 2009.
- 10 Kreidenweis, S., Koehler, K., DeMott, P., Prenni, A., Carrico, C., and Ervens, B.: Water activity and activation diameters from hygroscopicity data-Part I: Theory and application to inorganic salts, *Atmospheric Chemistry and Physics*, 5, 1357–1370, 2005.
- Mason, R. H., Si, M., Chou, C., Irish, V. E., Dickie, R., Elizondo, P., Wong, R., Brintnell, M., Elsasser, M., Lassar, W. M., Pierce, K. M., Leaitch, W. R., MacDonald, A. M., Platt, A., Toom-Sauntry, D., Sarda-Estève, R., Schiller, C. L., Suski, K. J., Hill, T. C. J., Abbatt, J. P. D., Huffman, J. A., DeMott, P. J., and Bertram, A. K.: Size-resolved measurements of ice-nucleating particles at six locations in North America and one in Europe, *Atmos. Chem. Phys.*, 16, 1637–1651, <https://doi.org/10.5194/acp-16-1637-2016>, <https://www.atmos-chem-phys.net/16/1637/2016/>, 2016.
- 15 McCluskey, C. S., Hill, T. C. J., Humphries, R. S., Rauker, A. M., Moreau, S., Stratton, P. G., Chambers, S. D., Williams, A. G., McRobert, I., Ward, J., Keywood, M. D., Harnwell, J., Ponsonby, W., Loh, Z. M., Krummel, P. B., Protat, A., Kreidenweis, S. M., and DeMott, P. J.: Observations of Ice Nucleating Particles Over Southern Ocean Waters, *Geophysical Research Letters*, 45, 11,989–11,997, <https://doi.org/10.1029/2018GL079981>, <https://doi.org/10.1029/2018GL079981>, 2018a.
- 20 McCluskey, C. S., Ovadnevaite, J., Rinaldi, M., Atkinson, J., Belosi, F., Ceburnis, D., Marullo, S., Hill, T. C. J., Lohmann, U., Kanji, Z. A., O’Dowd, C., Kreidenweis, S. M., and DeMott, P. J.: Marine and Terrestrial Organic Ice-Nucleating Particles in Pristine Marine to Continentally Influenced Northeast Atlantic Air Masses, *Journal of Geophysical Research: Atmospheres*, 123, 6196–6212, <https://doi.org/doi:10.1029/2017JD028033>, <https://agupubs.onlinelibrary.wiley.com/doi/abs/10.1029/2017JD028033>, 2018b.
- 25 Mertes, S., Verheggen, B., Walter, S., Connolly, P., Ebert, M., Schneider, J., Bower, K. N., Cozic, J., Weinbruch, S., Baltensperger, U., and Weingartner, E.: Counterflow Virtual Impactor Based Collection of Small Ice Particles in Mixed-Phase Clouds for the Physico-Chemical Characterization of Tropospheric Ice Nuclei: Sampler Description and First Case Study, *Aerosol Science and Technology*, 41, 848–864, <https://doi.org/10.1080/02786820701501881>, <https://doi.org/10.1080/02786820701501881>, 2007.
- Miles, N. L., Verlinde, J., and Clothiaux, E. E.: Cloud Droplet Size Distributions in Low-Level Stratiform Clouds, *Journal of the Atmospheric Sciences*, 57, 295–311, [https://doi.org/10.1175/1520-0469\(2000\)057<0295:cdsdil>2.0.co;2](https://doi.org/10.1175/1520-0469(2000)057<0295:cdsdil>2.0.co;2), <https://journals.ametsoc.org/doi/abs/10.1175/1520-0469%282000%29057%3C0295%3ACDSDIL%3E2.0.CO%3B2>, 2000.
- 30 Murray, B. J., O’Sullivan, D., Atkinson, J. D., and Webb, M. E.: Ice nucleation by particles immersed in supercooled cloud droplets, *Chemical Society Reviews*, 41, 6519–6554, <https://doi.org/10.1039/C2CS35200A>, <http://dx.doi.org/10.1039/C2CS35200A>, 2012.
- Niedermeier, D., Augustin-Bauditz, S., Hartmann, S., Wex, H., Ignatius, K., and Stratmann, F.: Can we define an asymptotic value for the ice active surface site density for heterogeneous ice nucleation?, *Journal of Geophysical Research: Atmospheres*, 120, 5036–5046, <https://doi.org/10.1002/2014JD022814>, <https://agupubs.onlinelibrary.wiley.com/doi/abs/10.1002/2014JD022814>, 2015.
- 35

- Niemand, M., Möhler, O., Vogel, B., Vogel, H., Hoose, C., Connolly, P., Klein, H., Bingemer, H., DeMott, P., Skrotzki, J., and Leisner, T.: A Particle-Surface-Area-Based Parameterization of Immersion Freezing on Desert Dust Particles, *Journal of the Atmospheric Sciences*, 69, 3077–3092, <https://doi.org/10.1175/jas-d-11-0249.1>, <http://journals.ametsoc.org/doi/abs/10.1175/JAS-D-11-0249.1>, 2012.
- O'Sullivan, D., Adams, M. P., Tarn, M. D., Harrison, A. D., Vergara-Temprado, J., Porter, G. C. E., Holden, M. A., Sanchez-Marroquin, A., Carotenuto, F., Whale, T. F., McQuaid, J. B., Walshaw, R., Hedges, D. H. P., Burke, I. T., Cui, Z., and Murray, B. J.: Contributions of biogenic material to the atmospheric ice-nucleating particle population in North Western Europe, *Scientific Reports*, 8, 13 821, <https://doi.org/10.1038/s41598-018-31981-7>, <https://doi.org/10.1038/s41598-018-31981-7>, 2018.
- Petters, M. and Wright, T.: Revisiting ice nucleation from precipitation samples, *Geophysical Research Letters*, 42, 8758–8766, <https://doi.org/doi:10.1002/2015GL065733>, <https://agupubs.onlinelibrary.wiley.com/doi/abs/10.1002/2015GL065733>, 2015.
- 10 Price, H. C., Baustian, K. J., McQuaid, J. B., Blyth, A., Bower, K. N., Choularton, T., Cotton, R. J., Cui, Z., Field, P. R., Gallagher, M., Hawker, R., Merrington, A., Miltenberger, A., Neely III, R. R., Parker, S. T., Rosenberg, P. D., Taylor, J. W., Trembath, J., Vergara-Temprado, J., Whale, T. F., Wilson, T. W., Young, G., and Murray, B. J.: Atmospheric Ice-Nucleating Particles in the Dusty Tropical Atlantic, *Journal of Geophysical Research: Atmospheres*, 123, 2175–2193, <https://doi.org/doi:10.1002/2017JD027560>, <https://agupubs.onlinelibrary.wiley.com/doi/abs/10.1002/2017JD027560>, 2018.
- 15 Pruppacher, H. and Klett, J.: *Microphysics of Clouds and Precipitation*, vol. 18, Springer Science & Business Media, 2010.
- Pummer, B. G., Budke, C., Augustin-Bauditz, S., Niedermeier, D., Felgitsch, L., Kampf, C. J., Huber, R. G., Liedl, K. R., Loerting, T., Moschen, T., Schauerperl, M., Tollinger, M., Morris, C. E., Wex, H., Grothe, H., Pöschl, U., Koop, T., and Fröhlich-Nowoisky, J.: Ice nucleation by water-soluble macromolecules, *Atmos. Chem. Phys.*, 15, 4077–4091, <https://doi.org/10.5194/acp-15-4077-2015>, <https://www.atmos-chem-phys.net/15/4077/2015/>, 2015.
- 20 Quinn, P. K., Collins, D. B., Grassian, V. H., Prather, K. A., and Bates, T. S.: Chemistry and Related Properties of Freshly Emitted Sea Spray Aerosol, *Chemical Reviews*, 115, 4383–4399, <https://doi.org/10.1021/cr500713g>, <http://dx.doi.org/10.1021/cr500713g>, 2015.
- Rangno, A. L. and Hobbs, P. V.: Microstructures and precipitation development in cumulus and small cumulonimbus clouds over the warm pool of the tropical Pacific Ocean, *Quarterly Journal of the Royal Meteorological Society*, 131, 639–673, <https://doi.org/10.1256/qj.04.13>, <https://rmets.onlinelibrary.wiley.com/doi/abs/10.1256/qj.04.13>, 2005.
- 25 Robinson, T. B., Stolle, C., and Wurl, O.: Depth is Relative: The Importance of Depth on TEP in the Near Surface Environment, *Ocean Sci. Discuss.*, 2019, 1–20, <https://doi.org/10.5194/os-2019-79>, <https://www.ocean-sci-discuss.net/os-2019-79/>, 2019.
- Schnell, R. C.: Ice Nuclei in Seawater, Fog Water and Marine Air off the Coast of Nova Scotia: Summer 1975, *Journal of the Atmospheric Sciences*, 34, 1299–1305, [https://doi.org/doi:10.1175/1520-0469\(1977\)034<1299:INISFW>2.0.CO;2](https://doi.org/doi:10.1175/1520-0469(1977)034<1299:INISFW>2.0.CO;2), <http://journals.ametsoc.org/doi/abs/10.1175/1520-0469%281977%29034%3C1299%3AINISFW%3E2.0.CO%3B2>, 1977.
- 30 Schnell, R. C. and Vali, G.: Biogenic Ice Nuclei: Part I. Terrestrial and Marine Sources, *Journal of the Atmospheric Sciences*, 33, 1554–1564, [https://doi.org/doi:10.1175/1520-0469\(1976\)033<1554:BINPIT>2.0.CO;2](https://doi.org/doi:10.1175/1520-0469(1976)033<1554:BINPIT>2.0.CO;2), <http://journals.ametsoc.org/doi/abs/10.1175/1520-0469%281976%29033%3C1554%3ABINPIT%3E2.0.CO%3B2>, 1976.
- Schrod, J., Weber, D., Drücke, J., Keleshis, C., Pikridas, M., Ebert, M., Cvetković, B., Nickovic, S., Marinou, E., Baars, H., Ansmann, A., Vrekoussis, M., Mihalopoulos, N., Sciare, J., Curtius, J., and Bingemer, H. G.: Ice nucleating particles over the Eastern Mediterranean measured by unmanned aircraft systems, *Atmos. Chem. Phys.*, 17, 4817–4835, <https://doi.org/10.5194/acp-17-4817-2017>, <https://www.atmos-chem-phys.net/17/4817/2017/>, 2017.
- Si, M., Irish, V. E., Mason, R. H., Vergara-Temprado, J., Hanna, S. J., Ladino, L. A., Yakobi-Hancock, J. D., Schiller, C. L., Wentzell, J. J. B., Abbatt, J. P. D., Carslaw, K. S., Murray, B. J., and Bertram, A. K.: Ice-nucleating ability of aerosol particles and possible sources at three

- coastal marine sites, *Atmos. Chem. Phys.*, 18, 15 669–15 685, <https://doi.org/10.5194/acp-18-15669-2018>, <https://www.atmos-chem-phys.net/18/15669/2018/>, 2018.
- Siebert, H. and Shaw, R. A.: Supersaturation Fluctuations during the Early Stage of Cumulus Formation, *Journal of the Atmospheric Sciences*, 74, 975–988, <https://doi.org/10.1175/jas-d-16-0115.1>, <https://journals.ametsoc.org/doi/abs/10.1175/JAS-D-16-0115.1>, 2017.
- 5 Suski, K. J., Hill, T. C. J., Levin, E. J. T., Miller, A., DeMott, P. J., and Kreidenweis, S. M.: Agricultural harvesting emissions of ice-nucleating particles, *Atmos. Chem. Phys.*, 18, 13 755–13 771, <https://doi.org/10.5194/acp-18-13755-2018>, <https://www.atmos-chem-phys.net/18/13755/2018/>, 2018.
- Tobo, Y., Prenni, A. J., DeMott, P. J., Huffman, J. A., McCluskey, C. S., Tian, G., Pöhlker, C., Pöschl, U., and Kreidenweis, S. M.: Biological aerosol particles as a key determinant of ice nuclei populations in a forest ecosystem, *Journal of Geophysical Research: Atmospheres*, 118, 10,100–10,110, <https://doi.org/10.1002/jgrd.50801>, <http://dx.doi.org/10.1002/jgrd.50801>, 2013.
- 10 Ullrich, R., Hoose, C., Möhler, O., Niemand, M., Wagner, R., Höhler, K., Hiranuma, N., Saathoff, H., and Leisner, T.: A New Ice Nucleation Active Site Parameterization for Desert Dust and Soot, *Journal of the Atmospheric Sciences*, 74, 699–717, <https://doi.org/10.1175/JAS-D-16-0074.1>, 2017.
- Vali, G.: Sizes of Atmospheric Ice Nuclei, *Nature*, 212, 384–385, <https://doi.org/10.1038/212384a0>, <https://doi.org/10.1038/212384a0>, 1966.
- 15 Vali, G.: Quantitative Evaluation of Experimental Results on the Heterogeneous Freezing Nucleation of Supercooled Liquids, *Journal of the Atmospheric Sciences*, 28, 402–409, [https://doi.org/10.1175/1520-0469\(1971\)028<0402:qeoea>2.0.co;2](https://doi.org/10.1175/1520-0469(1971)028<0402:qeoea>2.0.co;2), <http://journals.ametsoc.org/doi/abs/10.1175/1520-0469%281971%29028%3C0402%3AQEOERA%3E2.0.CO%3B2>, 1971.
- Vali, G., DeMott, P. J., Möhler, O., and Whale, T. F.: Technical Note: A proposal for ice nucleation terminology, *Atmos. Chem. Phys.*, 15, 10 263–10 270, <https://doi.org/10.5194/acp-15-10263-2015>, <https://www.atmos-chem-phys.net/15/10263/2015/>, 2015.
- 20 van Pinxteren, M., Barthel, S., Fomba, K. W., Müller, K., Von Tümping, W., and Herrmann, H.: The influence of environmental drivers on the enrichment of organic carbon in the sea surface microlayer and in submicron aerosol particles—measurements from the Atlantic Ocean, *Elementa: Science of the Anthropocene*, 5, 35, 2017.
- Welti, A., Müller, K., Fleming, Z. L., and Stratmann, F.: Concentration and variability of ice nuclei in the subtropical maritime boundary layer, *Atmospheric Chemistry and Physics*, 18, 5307–5320, 2018.
- 25 Westbrook, C. D. and Illingworth, A. J.: The formation of ice in a long-lived supercooled layer cloud, *Quarterly Journal of the Royal Meteorological Society*, 139, 2209–2221, <https://doi.org/10.1002/qj.2096>, <https://rmets.onlinelibrary.wiley.com/doi/abs/10.1002/qj.2096>, 2013.
- Wex, H., Huang, L., Zhang, W., Hung, H., Traversi, R., Becagli, S., Sheesley, R. J., Moffett, C. E., Barrett, T. E., Bossi, R., Skov, H., Hünerbein, A., Lubitz, J., Löffler, M., Linke, O., Hartmann, M., Herenz, P., and Stratmann, F.: Annual variability of ice-nucleating particle concentrations at different Arctic locations, *Atmos. Chem. Phys.*, 19, 5293–5311, <https://doi.org/10.5194/acp-19-5293-2019>, <https://www.atmos-chem-phys.net/19/5293/2019/>, 2019.
- 30 Wilson, T. W., Ladino, L. A., Alpert, P. A., Breckels, M. N., Brooks, I. M., Browse, J., Burrows, S. M., Carslaw, K. S., Huffman, J. A., Judd, C., Kilhau, W. P., Mason, R. H., McFiggans, G., Miller, L. A., Najera, J. J., Polishchuk, E., Rae, S., Schiller, C. L., Si, M., Temprado, J. V., Whale, T. F., Wong, J. P. S., Wurl, O., Yakobi-Hancock, J. D., Abbatt, J. P. D., Aller, J. Y., Bertram, A. K., Knopf, D. A., and Murray, B. J.: A marine biogenic source of atmospheric ice-nucleating particles, *Nature*, 525, 234–238, <https://doi.org/10.1038/nature14986>, <http://dx.doi.org/10.1038/nature14986>, 2015.

Characterization of aerosol particles at Cape Verde close to sea and cloud level heights - Part 2: ice nucleating particles in air, cloud and seawater

Xianda Gong¹, Heike Wex¹, Manuela van Pinxteren¹, Nadja Triesch¹, Khanneh Wadinga Fomba¹, Jasmin Lubitz¹, Christian Stolle^{2,3}, Tiera-Brandy Robinson³, Thomas Müller¹, Hartmut Herrmann¹, and Frank Stratmann¹

¹Leibniz Institute for Tropospheric Research, Leipzig, Germany

²Leibniz-Institute for Baltic Sea Research Warnemünde (IOW), Rostock, Germany

³Institute for Chemistry and Biology of the Marine Environment, University of Oldenburg, Wilhelmshaven, Germany

Correspondence: Xianda Gong (gong@tropos.de)

S1 Seawater samples

Table S1. The information of seawater samples at OS, including sample number, start time, end time, location, salinity, sodium chloride (NaCl) mass concentration, PH value and water temperature.

Sample Number	Start Time yyyy/mm/dd hh:mm:ss	End Time yyyy/mm/dd hh:mm:ss	Location	Salinity [g L ⁻¹]	NaCl [g L ⁻¹]	PH value	Temperature [°C]
SML01	2017/09/18 12:35:00	2017/09/18 13:00:00	-	-	-	-	-
ULW01	2017/09/18 12:35:00	2017/09/18 13:00:00	-	34.1	29.23	8.14	25.0
SML02	2017/09/20 09:32:00	2017/09/20 10:54:00	16°53'20 N, 24°54'22 W	36.2	31.03	8.11	26.7
ULW02	2017/09/20 09:32:00	2017/09/20 10:54:00	16°53'20 N, 24°54'22 W	36.3	31.11	8.12	26.7
SML03	2017/09/25 10:45:00	2017/09/25 11:48:00	16°53'46 N, 24°54'19 W	36.4	31.20	8.14	25.5
ULW03	2017/09/25 10:45:00	2017/09/25 11:48:00	16°53'46 N, 24°54'19 W	36.4	31.20	8.15	26.0
SML04	2017/09/26 11:05:00	2017/09/26 11:51:00	16°53'50 N, 24°54'27 W	36.1	30.94	8.12	26.4
ULW04	2017/09/26 11:05:00	2017/09/26 11:51:00	16°53'50 N, 24°54'27 W	36.3	31.11	8.15	25.1
SML05	2017/09/27 09:50:00	2017/09/27 11:00:00	16°53'38 N, 24°54'16 W	36.3	31.11	8.15	23.7
ULW05	2017/09/27 09:50:00	2017/09/27 11:00:00	16°53'38 N, 24°54'16 W	36.4	31.20	8.14	24.0
SML09	2017/10/04 09:15:00	2017/10/04 10:00:00	-	-	-	-	-
ULW09	2017/10/04 09:15:00	2017/10/04 10:00:00	-	36.2	31.03	8.23	23.7
SML12	2017/10/07 10:22:00	2017/10/07 11:35:00	16°53'25 N, 24°54'18 W	36.7	31.46	8.22	21.2
ULW12	2017/10/07 10:22:00	2017/10/07 11:35:00	16°53'25 N, 24°54'18 W	36.4	31.20	8.22	21.8
SML13	2017/10/09 09:30:00	2017/10/09 10:17:00	16°53'42 N, 24°54'08 W	36.6	31.37	8.19	21.5
ULW13	2017/10/09 09:30:00	2017/10/09 10:17:00	16°53'42 N, 24°54'08 W	36.4	31.20	8.13	23.6
SML14	2017/10/10 09:30:00	2017/10/10 10:30:00	16°53'43 N, 24°54'13 W	36.4	31.20	8.19	21.7
ULW14	2017/10/10 09:30:00	2017/10/10 10:30:00	16°53'43 N, 24°54'13 W	36.3	31.11	8.18	22.4

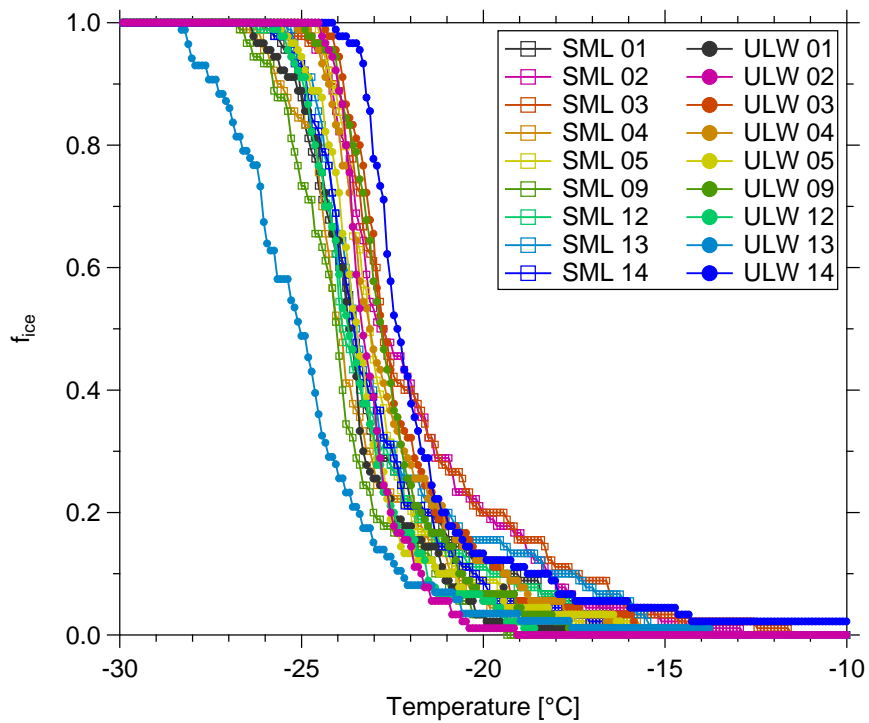


Figure S1. Frozen fraction (f_{ice}) measured by LINA as a function of temperature in SML and ULW. All temperatures have been corrected for freezing point depression.

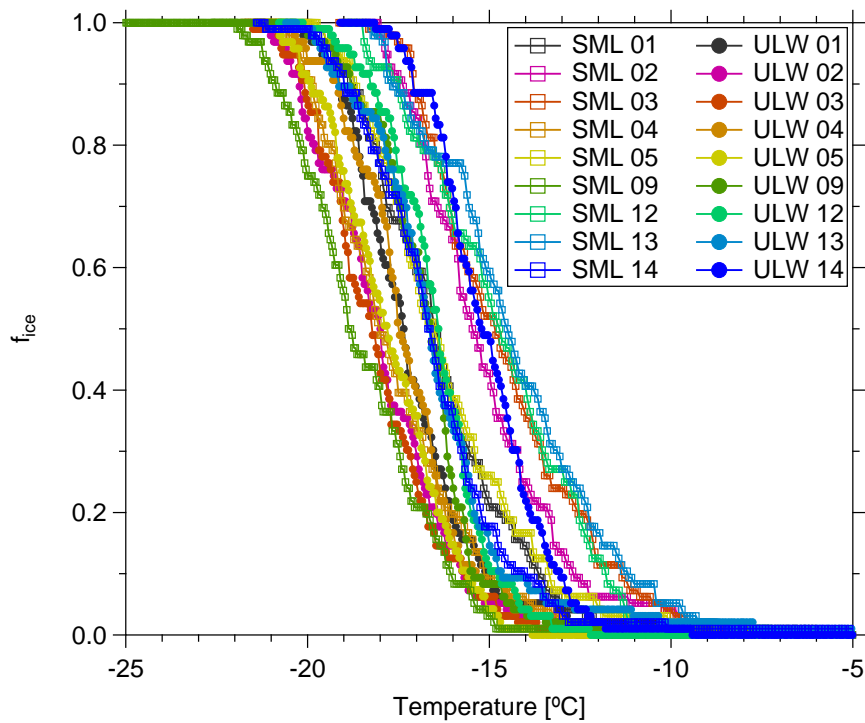


Figure S2. f_{ice} measured by INDA as a function of temperature in SML and ULW. All temperatures have been corrected for freezing point depression.

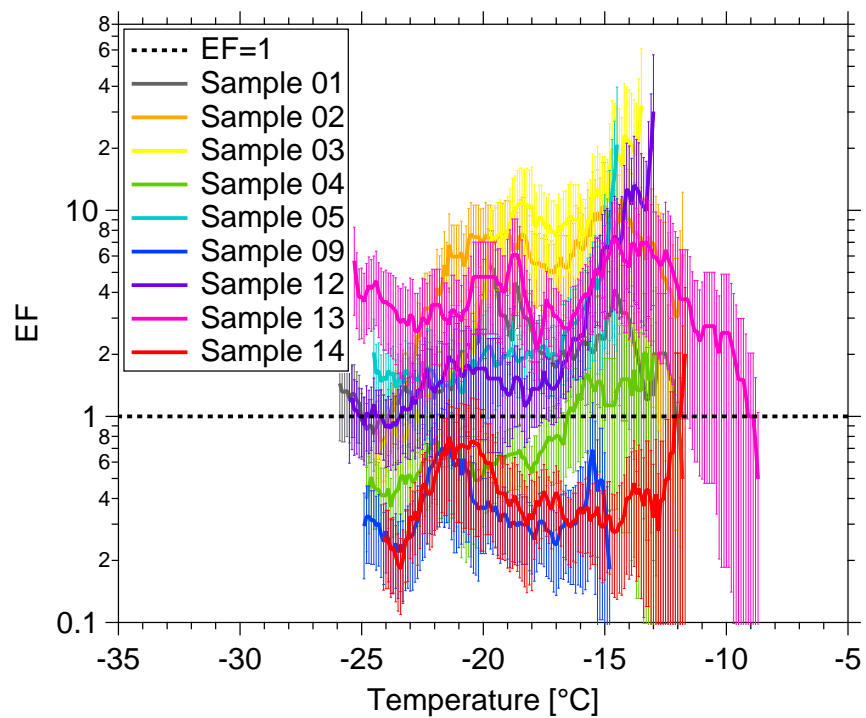


Figure S3. [EF as function of ice nucleation temperature. The EF=1 is shown by dashed line. Error bars show the measurement uncertainty.](#)

S2 Filter samples

S2.1 Background subtraction

N_{INP} from the field blanks was then subtracted from that of the filter samples, and the result was converted to background corrected atmospheric INP number concentrations, as the below equation shows:

$$5 \quad N_{\text{INP}} = (-\ln(1 - f_{\text{ice,s}}) + \ln(1 - f_{\text{ice,b}}))/V \quad (\text{S1})$$

The corrected atmospheric INP number concentration is N_{INP} , the frozen fractions measured for the filter samples and the field blanks are $f_{\text{ice,s}}$ and $f_{\text{ice,b}}$, respectively, and V is the volume of air sampled in each well.

S2.2 CVAO PM₁₀

Table S2. The information of PM₁₀ filter samples at CVAO, including sample number, start time, end time, duration, total sampling volume, sampling volume per well, sodium (Na⁺) and chloride (Cl⁻) mass concentration, total particle surface area concentration (A_{total}) and sample type.

Sample Number	Start Time yyyy/mm/dd hh:mm:ss	End Time yyyy/mm/dd hh:mm:ss	Duration [hminute]	Total Volume [std L ⁻¹ m ³]	Volume Per Well [std L ⁻¹]	Na ⁺ μg m ⁻³	Cl ⁻ μg m ⁻³	A_{total} μm ² cm ⁻³	Type
CVAO1583	2017/09/19 21:00:00	2017/09/20 21:00:00	1439.34	660.289	33.6882	4.40	6.19	370	PM ₁₀
CVAO1585	2017/09/22 16:00:00	2017/09/23 16:00:00	1439.34	660.289	33.6882	3.09	4.97	89	PM ₁₀
CVAO1586	2017/09/23 16:00:00	2017/09/24 16:00:00	1439.34	660.289	33.6882	2.36	3.36	78	PM ₁₀
CVAO1587	2017/09/24 16:00:00	2017/09/25 16:00:00	1439.34	660.289	33.6882	2.83	3.54	158	PM ₁₀
CVAO1588	2017/09/25 16:00:00	2017/09/26 16:00:00	1438.90	660.792	33.7139	3.32	4.98	277	PM ₁₀
CVAO1589	2017/09/26 16:00:00	2017/09/27 16:00:00	1439.61	661.462	33.7481	1.41	1.99	159	PM ₁₀
CVAO1590	2017/09/27 16:00:00	2017/09/28 16:00:00	1439.71	661.644	33.7573	1.77	2.70	198	PM ₁₀
CVAO1591	2017/09/28 16:00:00	2017/09/29 16:00:00	1439.73	661.420	33.7459	5.04	8.41	325	PM ₁₀
CVAO1592	2017/09/29 16:00:00	2017/09/30 16:00:00	1439.73	660.289	33.6882	6.49	11.26	297	PM ₁₀
CVAO1593	2017/09/30 16:00:00	2017/10/01 16:00:00	1439.73	660.821	33.7153	5.32	8.99	238	PM ₁₀
CVAO1594	2017/09/29 16:00:00	2017/09/30 16:00:00							Blind filter
CVAO1595	2017/10/01 16:00:00	2017/10/02 16:00:00	1439.36	659.330	33.6393	4.52	6.67	172	PM ₁₀
CVAO1596	2017/10/02 16:00:00	2017/10/03 16:00:00	1439.71	660.629	33.7056	3.71	6.49	171	PM ₁₀
CVAO1597	2017/10/03 16:00:00	2017/10/04 16:00:00	1439.71	660.629	33.7056	-	-	169	PM ₁₀
CVAO1598	2017/10/05 16:00:00	2017/10/06 16:00:00	1439.55	659.264	33.6359	2.58	3.33	162	PM ₁₀
CVAO1641	2017/10/06 16:00:00	2017/10/07 16:00:00	1439.73	658.670	33.6056	4.67	6.91	244	PM ₁₀
CVAO1642	2017/10/07 16:00:00	2017/10/08 16:00:00	1439.71	661.187	33.7341	5.46	8.54	271	PM ₁₀
CVAO1643	2017/10/08 16:00:00	2017/10/09 16:00:00	1439.71	659.785	33.6625	5.22	7.98	230	PM ₁₀
CVAO1644	2017/10/07 17:00:00	2017/10/08 17:00:00							Blind filter

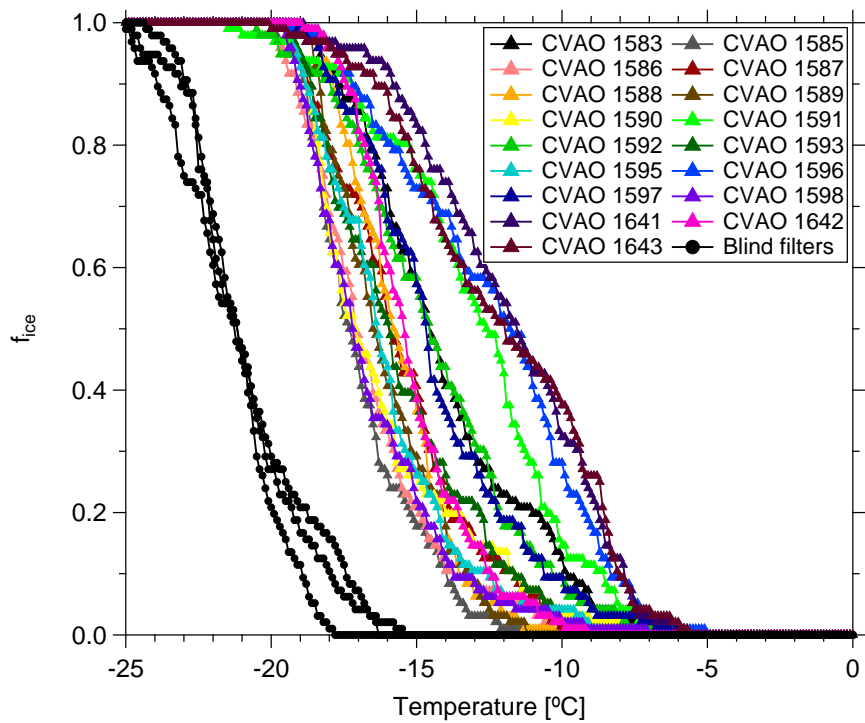


Figure S4. f_{ice} measured by INDA (without background subtraction) as a function of temperature in CVAO PM₁₀ filters. f_{ice} of blind filters are shown by black dots.

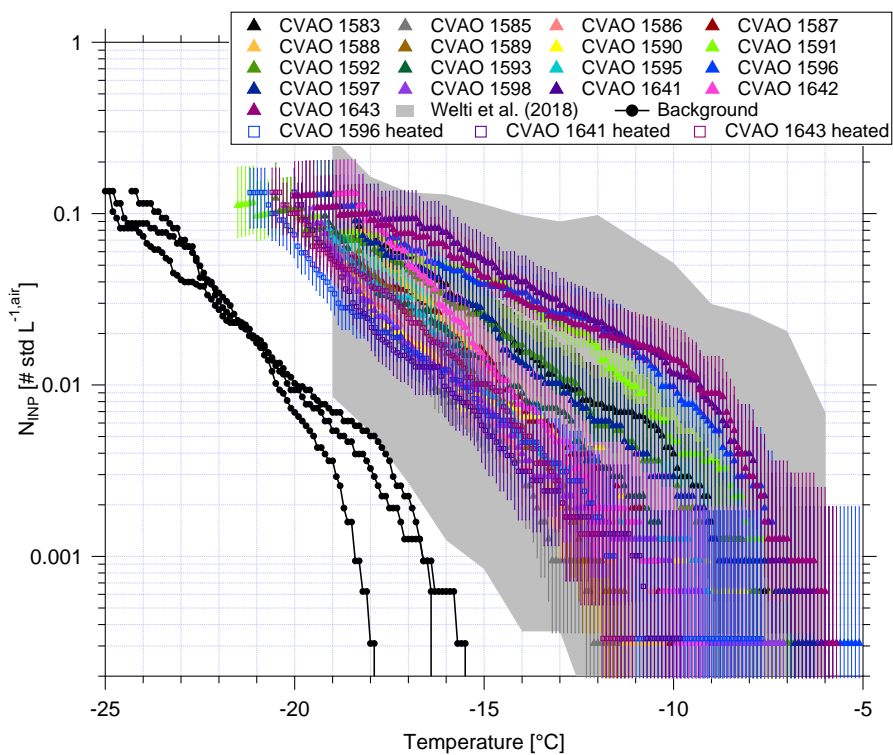


Figure S5. N_{INP} as a function of temperature from CVAO PM₁₀ filters. The field measurement of N_{INP} in PM₁₀ by Welte et al. (2018) is shown by gray shadow. Error bars show the 95% confidence interval. Black dots show the measurement background.

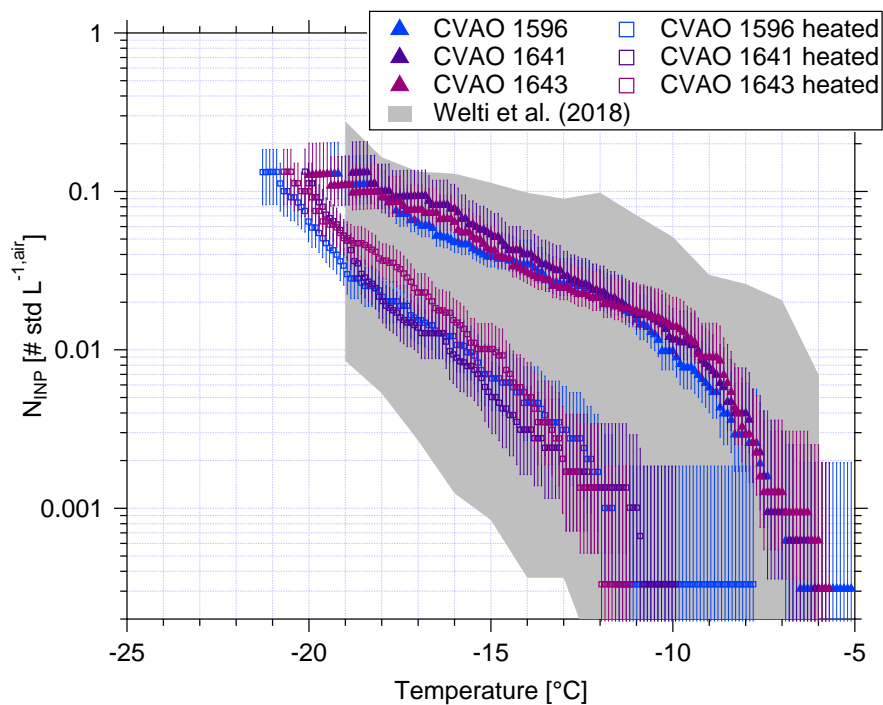


Figure S6. Comparison of N_{INP} as a function of temperature from CVAO 1596, CVAO 1641 and CVAO 1643 before and after heating (CVAO PM_{10} filters). The field measurement of N_{INP} in PM_{10} by Welti et al. (2018) is shown by gray shadow. Error bars show the 95% confidence interval. Background correction is included for all filter samples.

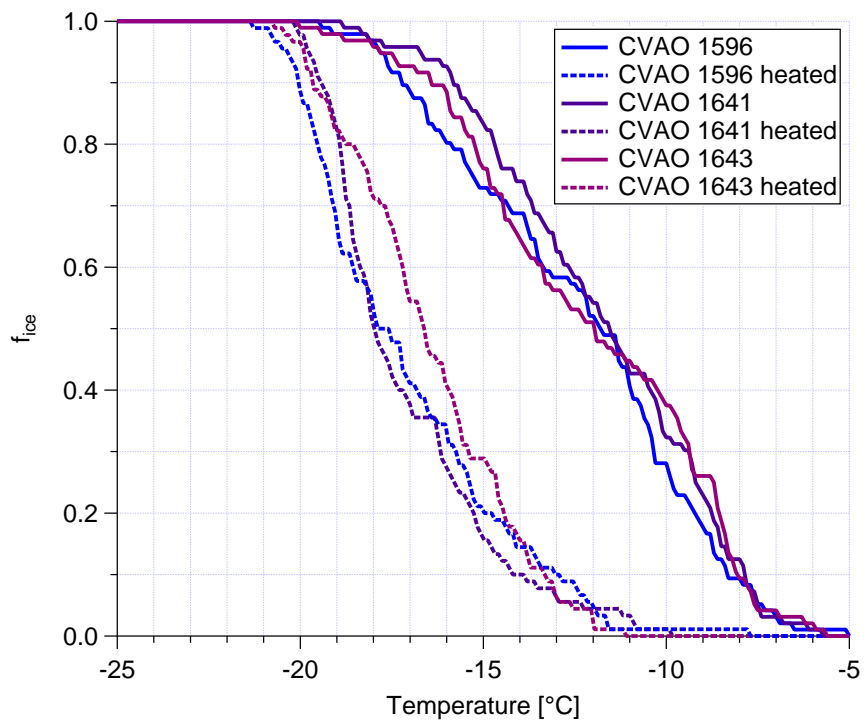


Figure S7. Comparison of f_{ice} measured by INDA (without background subtraction) as a function of temperature from CVAO 1596, CVAO 1641 and CVAO 1643 before and after heating (CVAO PM₁₀ filters).

S2.3 CVAO PM₁

Table S3. The information of PM₁ filter samples at CVAO, including sample number, start time, end time, duration, total sampling volume, sampling volume per well and sample type.

Sample Number	Start Time yyyy/mm/dd hh:mm:ss	End Time yyyy/mm/dd hh:mm:ss	Duration [hminute]	Total Volume [std L ⁻¹ m ³]	Volume Per Well [std L ⁻¹]	Type
CVAO924	2017/09/19 21:00:00	2017/09/20 21:00:00	1439.36	661.200	33.7347	PM ₁
CVAO925	2017/09/21 21:00:00	2017/09/22 21:00:00	1439.36	661.200	33.7347	PM ₁
CVAO926	2017/09/22 16:00:00	2017/09/23 16:00:00	1439.36	661.200	33.7347	PM ₁
CVAO927	2017/09/23 16:00:00	2017/09/24 16:00:00	1439.36	661.200	33.7347	PM ₁
CVAO928	2017/09/24 16:00:00	2017/09/25 16:00:00	1439.36	661.200	33.7347	PM ₁
CVAO929	2017/09/25 16:00:00	2017/09/26 16:00:00	1439.21	664.115	33.8834	PM ₁
CVAO930	2017/09/26 16:00:00	2017/09/27 16:00:00	1439.36	661.200	33.7347	PM ₁
CVAO931	2017/09/27 16:00:00	2017/09/28 16:00:00	1439.36	661.200	33.7347	PM ₁
CVAO932	2017/09/28 16:00:00	2017/09/29 16:00:00	1439.36	661.200	33.7347	PM ₁
CVAO933	2017/09/29 16:00:00	2017/09/30 16:00:00	1439.36	661.200	33.7347	PM ₁
CVAO934	2017/09/30 16:00:00	2017/10/01 16:00:00	1439.36	661.200	33.7347	PM ₁
CVAO935	2017/09/29 16:00:00	2017/09/30 16:00:00				Blind filter
CVAO936	2017/10/01 16:00:00	2017/10/02 16:00:00	1438.53	659.798	33.6632	PM ₁
CVAO937	2017/10/02 16:00:00	2017/10/03 16:00:00	1439.55	660.255	33.6865	PM ₁
CVAO938	2017/10/03 16:00:00	2017/10/04 16:00:00	1439.36	661.200	33.7347	PM ₁
CVAO939	2017/10/04 16:00:00	2017/10/05 16:00:00	1439.36	661.200	33.7347	PM ₁
CVAO940	2017/10/05 16:00:00	2017/10/06 16:00:00	1439.18	661.071	33.7281	PM ₁
CVAO941	2017/10/06 16:00:00	2017/10/07 16:00:00	1439.58	662.336	33.7927	PM ₁
CVAO942	2017/10/07 16:00:00	2017/10/08 16:00:00	1439.58	662.122	33.7817	PM ₁
CVAO944	2017/10/08 16:00:00	2017/10/09 16:00:00	1439.55	660.377	33.6927	PM ₁

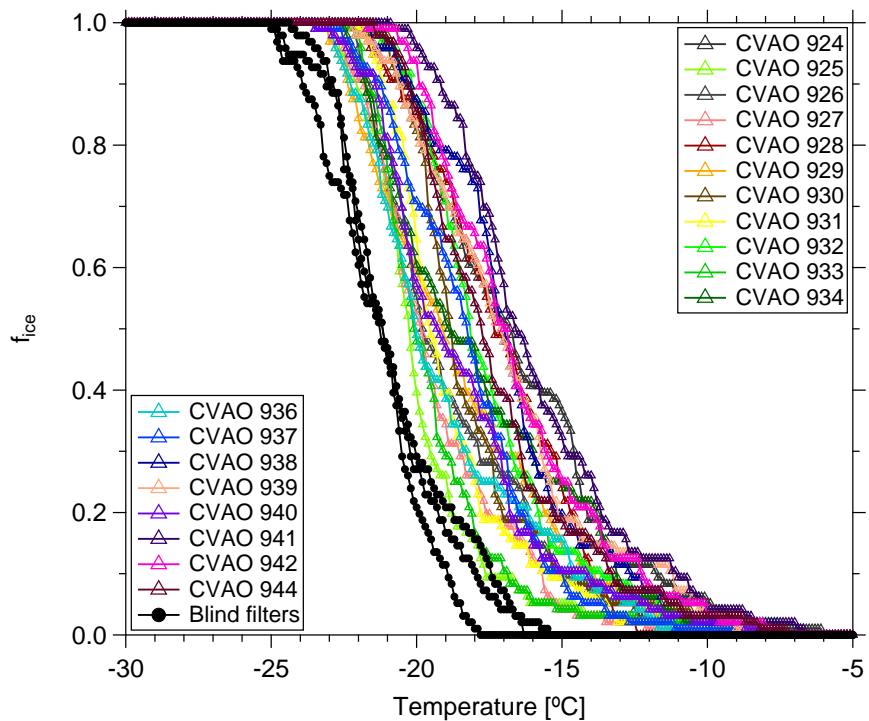


Figure S8. f_{ice} measured by INDA (without background subtraction) as a function of temperature in CVAO PM₁ filters. f_{ice} of blind filters are shown by black dots.

S2.4 MV PM₁₀

Table S4. The information of PM₁₀ filter samples at MV, including sample number, start time, end time, duration, total sampling volume, sampling volume per well, cloud time (percent of the time MV was in cloud during the filter was sampled) and sample type.

Sample Number	Start Time yyyy/mm/dd hh:mm:ss	End Time yyyy/mm/dd hh:mm:ss	Duration [hminute]	Total Volume [std L=1m ³]	Volume Per Well [std L=1]	Cloud time [%]	Type
MV1600	2017/09/21 16:39:00	2017/09/22 16:23:00	1382.86	601.870	30.7077	67.44%	PM ₁₀
MV1601	2017/09/22 16:23:00	2017/09/23 15:59:00	1418.31	615.998	31.4285	17.39%	PM ₁₀
MV1602	2017/09/23 15:59:00	2017/09/24 16:01:00	1440.60	625.035	31.8896	6.12%	PM ₁₀
MV1603	2017/09/24 16:01:00	2017/09/25 16:11:00	1449.61	629.660	32.1255	4.17%	PM ₁₀
MV1604	2017/09/25 16:13:00	2017/09/26 16:19:00	1444.90	627.655	32.0232	61.70%	PM ₁₀
MV1605	2017/09/26 16:20:00	2017/09/27 16:23:00	1440.58	627.381	32.0092	65.96%	PM ₁₀
MV1606	2017/09/27 16:23:00	2017/09/28 16:59:00	1464.99	637.541	32.5276	79.59%	PM ₁₀
MV1607	2017/09/28 17:01:00	2017/09/29 16:28:00	1406.21	611.922	31.2205	97.83%	PM ₁₀
MV1608	2017/09/29 16:30:00	2017/09/30 16:28:00	1676.36	760.265	38.7890	93.75%	PM ₁₀
MV1609	2017/10/01 19:02:00	2017/10/02 17:09:00	1326.63	576.405	29.4084	47.73%	PM ₁₀
MV1610	2017/10/02 17:09:00	2017/10/03 17:09:00	1439.36	624.715	31.8732	52.08%	PM ₁₀
MV1611	2017/10/03 17:10:00	2017/10/04 16:27:00	1396.11	606.390	30.9383	50.00%	PM ₁₀
MV1612	2017/10/04 16:27:00	2017/10/05 16:00:00	1408.61	613.421	31.2970	69.05%	PM ₁₀
MV1613	2017/10/05 16:00:00	2017/10/06 16:01:00	1441.46	627.486	32.0146	79.59%	PM ₁₀
MV1614	2017/10/06 16:03:00	2017/10/07 16:02:00	1439.46	625.832	31.9302	87.23%	PM ₁₀
MV1615	2017/10/07 16:02:00	2017/10/08 18:12:00	1439.36	627.485	32.0145	100.00%	PM ₁₀
MV1616	2017/10/08 18:13:00	2017/10/09 12:04:00	1071.60	467.526	23.8534	100.00%	PM ₁₀

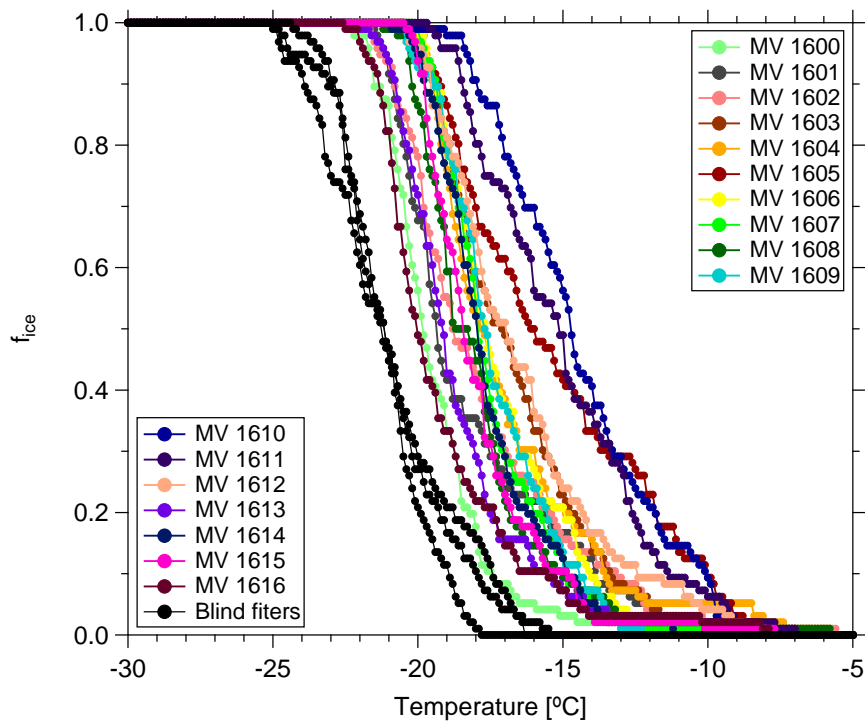


Figure S9. f_{ice} measured by INDA (without background subtraction) as a function of temperature in MV PM₁₀ filters. f_{ice} of blind filters are shown by black dots.

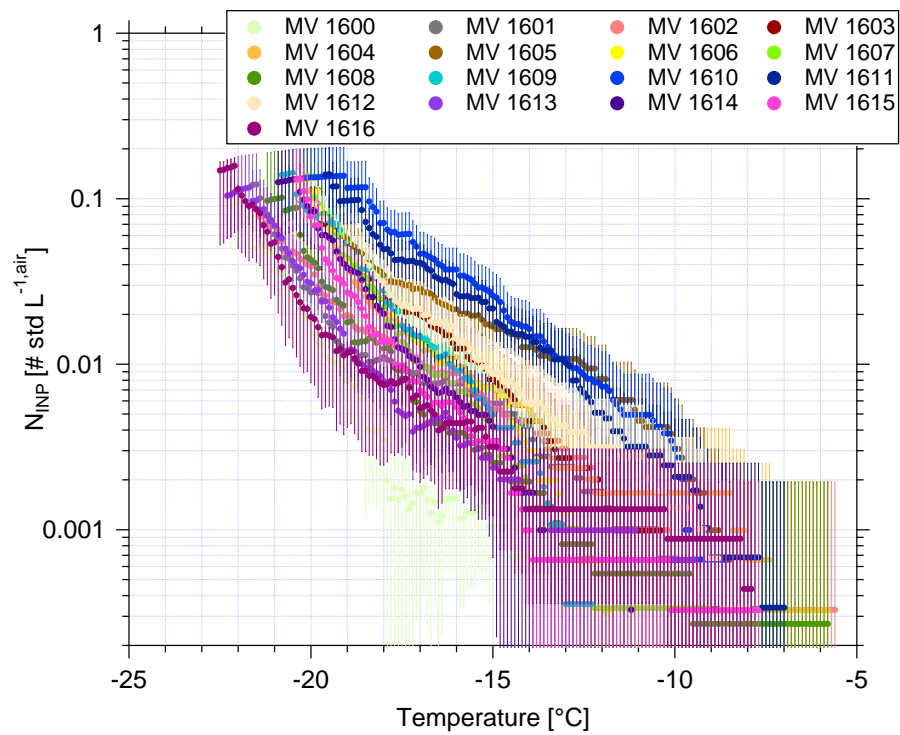


Figure S10. N_{INP} as function of temperature in MV PM₁₀ filters. N_{INP} are background-corrected. Error bars show the 95% confidence interval.

S3 Cloud samples

Table S5. The information of cloud water samples, including sample number, start time, end time, duration, volume, sodium (Na^+) and chloride (Cl^-) mass concentration and $N_{\text{CCN},0.30\%}$.

Sample Number	Start Time yyyy/mm/dd hh:mm:ss	End Time yyyy/mm/dd hh:mm:ss	Duration (h) [h]	Volume [mL]	Na^+ mg L^{-1}	Cl^- mg L^{-1}	$N_{\text{CCN},0.30\%}$ cm^{-3}
Cloud01	2017/09/20 13:25:00	2017/09/20 18:20:00	4.92	185	8.44	15.51	551
Cloud03	2017/09/26 19:00:00	2017/09/27 08:00:00	13.00	435	8.32	14.15	387
Cloud04	2017/09/27 19:00:00	2017/09/28 07:30:00	12.50	544	5.00	9.27	239
Cloud05	2017/09/28 19:00:00	2017/09/29 07:30:00	12.50	537	14.18	24.57	560
Cloud11	2017/10/04 19:00:00	2017/10/05 07:30:00	12.50	150	46.11	70.30	481
Cloud12	2017/10/05 07:45:00	2017/10/05 17:38:00	9.88	78	22.75	36.99	494
Cloud13	2017/10/05 17:40:00	2017/10/05 20:10:00	2.50	133	16.97	25.23	442
Cloud14	2017/10/05 20:10:00	2017/10/05 23:30:00	3.33	131	17.31	24.36	473
Cloud15	2017/10/05 23:30:00	2017/10/06 04:00:00	4.50	120	21.85	31.95	491
Cloud16	2017/10/06 04:05:00	2017/10/06 08:00:00	3.92	120	16.87	19.77	445
Cloud19	2017/10/06 18:00:00	2017/10/07 06:30:00	12.50	537	18.34	29.10	482
Cloud20	2017/10/07 06:48:00	2017/10/07 10:48:00	4.00	88	28.19	41.54	510
Cloud24	2017/10/08 19:00:00	2017/10/09 07:00:00	12.00	537	24.54	32.46	625

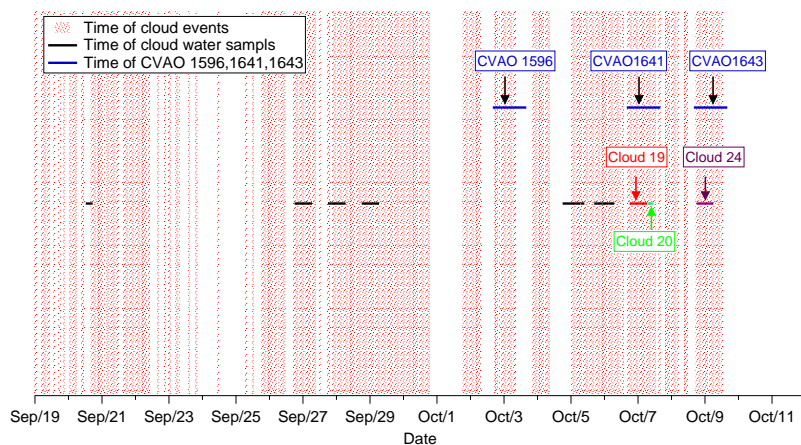


Figure S11. Times during which MV was in clouds (in red shadows) and the sampling time of all cloud water and that of some selected CVAO PM₁₀ filters.

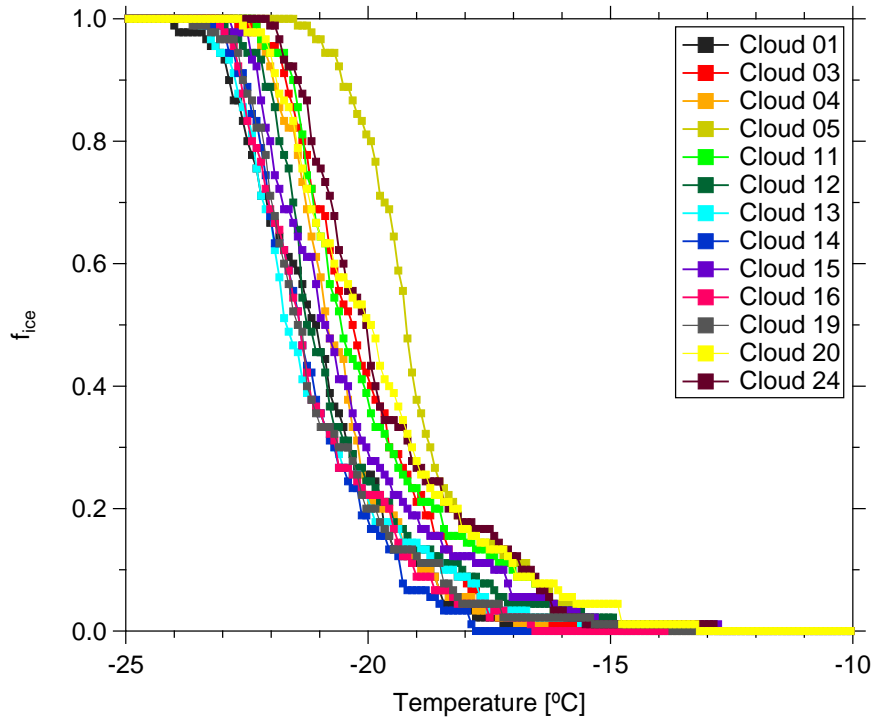


Figure S12. f_{ice} measured by LINA as a function of temperature in cloud water.

S4 Particle surface area size distribution

A thorough aerosol characterization has been done during the measurement campaign, and is described in detail in Gong et al. (2019). Fig. S14 shows the median particle surface area size distribution (PASD) for the whole campaign. Error bars show the 75th and 25th percentiles. Two different modes were observed, i.e., a small mode (30-500 nm) and a larger mode (500 nm-10 μm). The larger mode particle surface area is about 3 times higher than the small mode. Based on the PASD, the concentrations for the total surface area of the particles were calculated. The total particle surface area concentration (A_{total}) varied from 35 to 824 $\mu\text{m}^2 \text{cm}^{-3}$, with a median of 116 $\mu\text{m}^2 \text{cm}^{-3}$. The averaged A_{total} during each CVAO PM_{10} sampling period varied from 78 to 370 $\mu\text{m}^2 \text{cm}^{-3}$ (summarized in Tab. S2). Based on airborne measurements in the Saharan dust layer, Price et al. (2018) found A_{total} mainly above 100 with a maximum of 688 $\mu\text{m}^2 \text{cm}^{-3}$, which is higher than values found for this study, likely due to the fact that Cape Verde is at some distance to the Sahara and also that less strong dust events were sampled.

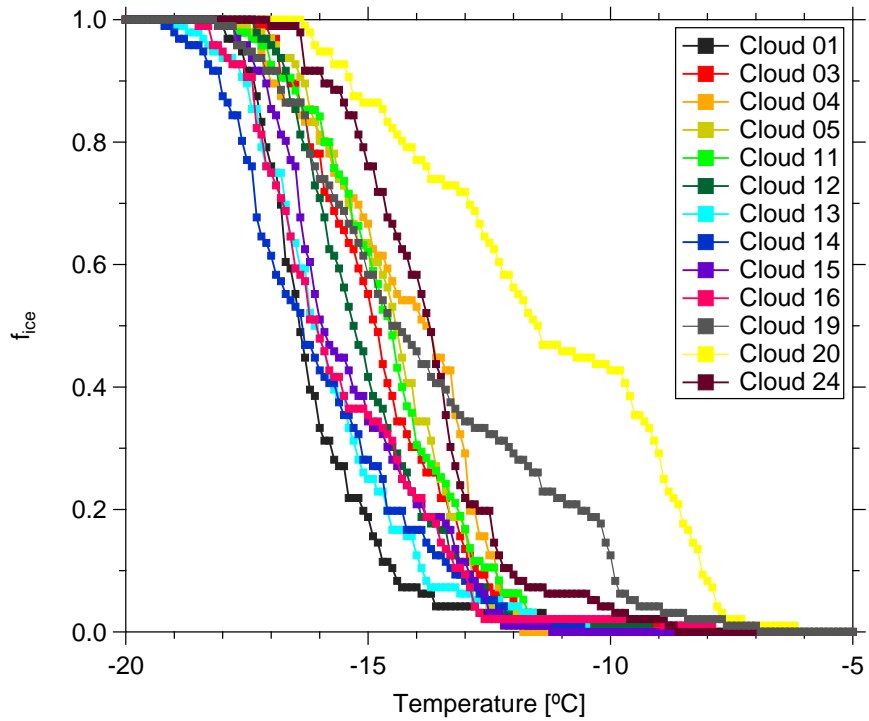


Figure S13. f_{ice} measured by INDA as a function of temperature in cloud water.

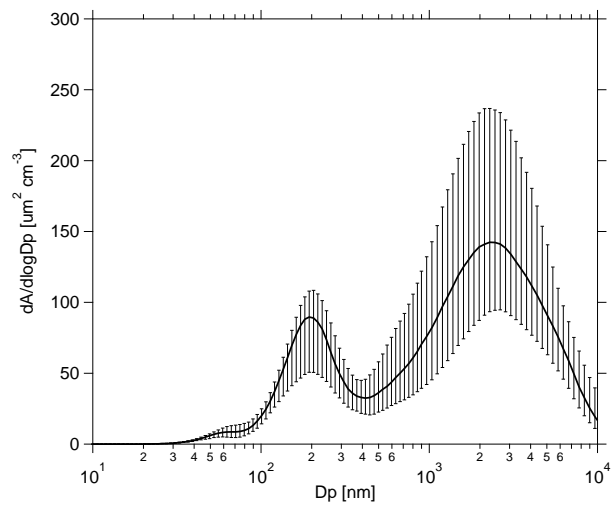


Figure S14. The median PASD during the whole campaign. The error bar indicates the range between the 75th and 25th percentiles.

References

- Gong, X., Wex, H., Voigtländer, J., Fomba, K. W., Weinhold, K., van Pinxteren, M., Henning, S., Müller, T., Herrmann, H., and Stratmann, F.: Characterization of aerosol particles at Cape Verde close to sea and cloud level heights – Part 1: particle number size distribution, cloud condensation nuclei and their origins, *Atmos. Chem. Phys. Discuss.*, 2019, 1–31, <https://doi.org/10.5194/acp-2019-585>, <https://www.atmos-chem-phys-discuss.net/acp-2019-585/>, 2019.
- 5 Price, H. C., Baustian, K. J., McQuaid, J. B., Blyth, A., Bower, K. N., Choularton, T., Cotton, R. J., Cui, Z., Field, P. R., Gallagher, M., Hawker, R., Merrington, A., Miltenberger, A., Neely III, R. R., Parker, S. T., Rosenberg, P. D., Taylor, J. W., Trembath, J., Vergara-Temprado, J., Whale, T. F., Wilson, T. W., Young, G., and Murray, B. J.: Atmospheric Ice-Nucleating Particles in the Dusty Tropical Atlantic, *Journal of Geophysical Research: Atmospheres*, 123, 2175–2193, <https://doi.org/doi:10.1002/2017JD027560>, <https://agupubs.onlinelibrary.wiley.com/doi/abs/10.1002/2017JD027560>, 2018.
- 10 Welti, A., Müller, K., Fleming, Z. L., and Stratmann, F.: Concentration and variability of ice nuclei in the subtropical maritime boundary layer, *Atmospheric Chemistry and Physics*, 18, 5307–5320, 2018.